INVESTIGATION OF THE IMPACT AND VIABILITY OF WHEELING RENEWABLE DISTRIBUTED GENERATION TO RESIDENTIAL LOADS OF GWARINPA HOUSING ESTATE, ABUJA

BY

ABDULLAHI, Baba Abdullahi
MEng/SEET/2018/8241

DEPARTMENT OF ELECTRICAL AND ELECTRONICS ENGINEERING,

FEDERAL UNIVERSITY OF TECHNOLOGY

MINNA

MAY, 2023

INVESTIGATION OF THE IMPACT AND VIABILITY OF WHEELING RENEWABLE DISTRIBUTED GENERATION TO RESIDENTIAL LOADS OF GWARINPA HOUSING ESTATE, ABUJA

BY

ABDULLAHI, Baba Abdullahi
MEng/SEET/2018/8241

A THESIS SUBMITTED TO THE POSTGRADUATE SCHOOL, FEDERAL UNIVERSITY OF TECHNOLOGY MINNA, NIGERIA IN PARTIAL FULFILLMENT OF THE REQUIREMENTS FOR THE AWARD OF THE DEGREE OF MASTER OF ENGINEERING (MEng) IN POWER SYSTEM ENGINEERING

MAY, 2023

DECLARATION

I hereby declare that this thesis titled: "**Investigation of the impact and viability of wheeling renewable distributed generation to residential loads of Gwarinpa housing estate, Abuja**" is a collection of my original research work and it has not been presented for any other qualification anywhere. Information from other sources (published or unpublished) has been duly acknowledged.

ABDULLAHI, Baba Abdullahi
MEng/SEET/2018/8241
FEDERAL UNIVERSITY OF TECHNOLOGY
MINNA, NIGERIA

…… SIGNATURE/DATE

CERTIFICATION

The thesis titled: "**Investigation of the impact and viability of wheeling renewable distributed generation to residential loads of Gwarinpa housing estate, Abuja**" by: ABDULLAHI, Baba Abdullahi (MEng/SEET/2018/8241) meets the regulations governing the award of the degree of Master of Engineering (MEng) of the Federal University of Technology, Minna and it is approved for its contribution to scientific knowledge and literary presentation.

ENGR. DR. L. J. OLATOMIWA ……...
MAJOR SUPERVISOR Signature & Date

ENGR. PROF. J. TSADO …...……..……..
CO-SUPERVISOR Signature & Date

ENGR. DR. L. J. OLATOMIWA …...…….……...
HEAD OF DEPARTMENT Signature & Date

ENGR. PROF. E. N. ONWUKA ……..…..……...
DEAN OF SCHOOL OF ELECTRICAL Signature & Date
ENGINEERING AND TECHNOLOGY

ENGR. PROF. O. K. ABUBAKRE …...…….……...
DEAN OF POSTGRADUATE SCHOOL Signature & Date

DEDICATION

I dedicate this document to my Family, Friends and well-wishers.

ACKNOWLEDGEMENTS

Without sound health, basic knowledge and financial resources, the desire to undertake this programme will remain a mirage. Therefore, all glory belongs to GOD, the Indisputable Creator, Sustainer and Taker of life.

Special appreciation to my parents for building a solid foundation upon which I stand to undertake this study. And to my siblings, thank you for the support and encouragement.

With great pleasure, I recognize my lovely wife, Hajiya Fatima Waziri, my children; Abdullahi, Fazila, Abdulrahman and Saratu, for their understanding to bear with the time and resources I had to share in undertaking this research study. To my sister-in-law, Hajiya Hauwa Waziri, thanks for the concern and regular prayers.

I wish to use this opportunity to acknowledge individuals and collective contributions made by Electrical and Electronics Engineering staff (academic and non-academic). To the supervisory team led by Dr. Lanre Olatomiwa, in collaboration with Prof. Jacob Tsado and the internal examiner, Dr. Ahmad Sadiq Abubakar, I will not be tired of thanking you for the guidance and criticism that produced this thesis. Furthermore, I wish to appreciate the unrelenting push and words of encouragement from my lead supervisor. This, and the grace of GOD, kept me moving against retrogressive forces.

To our able postgraduate coordinator, Dr. O. J. Tola, for the regular counselling and encouragement. To my friend-cum-brother, Dr. U.S Dauda, thanks for your time, effort, and knowledge, which made this work a whole lot easier. I wish to thank Dr. J. Ambafi, and others, not mentioned, for their input and brotherly counselling. May God bless you all.

ABSTRACT

With a national peak demand forecast of 28,850 MW against the grid generation installed capacity of 13,014.14 MW, Nigeria's electricity suffer power supply deficit. The residential sector, which accounts for about 60 % of electricity consumption, is the worst hit. Energy wheeling, a system of transporting distributed generation from an Independent Power Producer (IPP) to industrial consumers via the utility's distribution network, is one of the emerging systems of power sector deregulation, capable of improving supply to residential consumers under power purchase agreements. This research examined the impact of energy wheeling from renewable Distributed Generation (DG) to diverse and stochastic characteristics of residential loads via the existing 9-bus distribution network of Gwarinpa housing estate Abuja to determine its viability. Two software packages, Hybrid optimization for multiple energy resources (HOMER) and digital simulation of electrical networks (DIgSILENT), were used to determine the renewable energy potential for the estate and the impact of energy wheeling on voltage profile, fault level, losses and thermal loading of the distribution network respectively. The result shows an optimal grid/PV/converter configuration with a Levelized Cost of Electricity (LCOE) of $0.0188 and Net Present Cost (NPC) of $72.4 million. The load flow of the PV-connected distribution network produced 6.38 % improvement in voltage profile of the critical bus 7 and 8, 88.57 % reduction in thermal loading and 98 % reduction in reactive power losses respectively, of the erstwhile overloaded line 2. Fault levels were unchanged with the integration of the inverter-based PV systems. Therefore, based on conformity of the results to established power distribution system technical specifications and the grid code for the Nigeria power system, energy wheeling from renewable DG to diverse and stochastic residential loads via the utility distribution network is practicable and viable.

TABLE OF CONTENTS

LIST OF TABLES

LIST OF FIGURES

ABBREVIATIONS

BESS	Battery Energy Storage Systems
BOT	Build, Operate and Transfer
CdTe	Cadmium Telluride
CIGS	Copper Indium Gallium Selenide
CUF	Capacity Utilization Factor
DG	Distributed Generation
DIgSILENT	Digital Simulation of Electrical Network
EPSRA	Electricity Power Sector Reform Act
GHE	Gwarinpa Housing Estate
GHI	Global Horizontal Irradiance
HAWT	Horizontal Axis Wind Turbine
HOMER	Hybrid Optimization of Multiple Energy Resources
HRES	Hybrid Renewable Energy System
IEA	International Energy Agency
IRENA	International Renewable Energy Agency
IPP	Independent Power Producer
kV	kiloVolt
kW/m^2	KiloWatt per square Metre
LCOE	Levelized Cost of Electricity
LOLP	Loss of Load Probability
LPSP	Loss of Power Supply Probability
MW	Megawatt
MVAR	MegaVolt-Ampere Reactive
NESI	Nigeria Electricity Supply Industry

NPC	Net Present Cost
NREL	National Renewable Energy Laboratory
PV	PhotoVoltaic
SPL	System Performance Level
VAWT	Vertical Axis Wind Turbine

CHAPTER ONE

1.0 INTRODUCTION

1.1 Background to the Study

According to the National Bureau of Statistics, Nigeria is the most populated country in Africa and the seventh most populated in the world, with a population estimate of 208 million people (Olanrewaju *et al.*, 2020). Nigeria's electricity-consuming population is grouped into three (3) sectors; the residential, commercial, and industrial sectors (Babatunde and Shuaibu, 2009). The residential sector accounts for 60 %, followed by the commercial sector (Olaniyan *et al.*, 2018). Since population, among other variables such as the gross domestic product, relates to electricity consumption (Kavaklioglu, 2019; To *et al.*, 2017), the demand for power supply is expected to be high, and thus the power generated.

Before the Nigerian power sector deregulation, the National Electric Power Authority (NEPA), a state-owned, vertically integrated utility company, controlled the nation's power generation, transmission and distribution systems. The country has a grid generation installed capacity of 13,014.14 MW, a generation capacity of 7,652.6 MW and a peak generated value of 5,801.60 MW. The transmission wheeling capacity is 8,100 MW, and an average sent-out energy of 3,971 MWH in 2018. The current access rate stood at 45 %, with 55 % for urban and 36 % for rural areas. While the energy consumption per capita was 129 kWh per annum (Momoh, 2019). Furthermore, electricity accounts for 2 % of the total final energy consumption in Nigeria, and 9 % of the household's total energy consumption. Thus, after many years of monopoly in the power business, consumers were still faced with the shortage of electricity supply and

estimated billing. On the other hand, the power system suffered losses, financial constraints, and energy theft (Emovon *et al.*, 2018).

To find a solution to the challenges mentioned above, the Electric Power Sector Reform (EPSR) Act was enacted in 2005 to attract private investors to the business of power. Private investors eventually took over the generation and distribution sectors in September 2013 (Idowu *et al.*, 2019). However, the gap between the demand and supply of electricity in Nigeria remains wide and contributes to incessant power outage to consumers, particularly the residential, which consumes most of the power generated (Babatunde and Shuaibu, 2009). The government-owned Independent System Operator (ISO) made a National Peak Demand forecast of 28,850.00 MW. Still, it is estimated that about 60,000 MW is required for a stable power supply which could be achieved by a substantial mix of renewable energy (Olaoye *et al.*, 2016). Though long ago, consumers adopted renewable energy options to self-generate electricity. A cost-effective alternative approach of securing power from DG of Independent Power Producers (IPP) via the existing grid network is the wheeling approach (Murray, 2018).

As it is popularly known, energy wheeling entails a power purchase agreement between an IPP, a willing buyer, and the utility grid provider. This system is being practiced successfully in deregulated systems in Britain, New Zealand, Spain, Chile, Argentina, India and so on, and has contributed to reducing the cost of electricity (Baji and Ashok, 1998; Happ, 1994). The system unlocks stranded power capacity and renewable potential and encourages investment into independent power production (Murray, 2018).

With deregulation, there will be a paradigm shift away from a centralized system. DG refers to electricity generation, usually small-scale, at or near end users

(El-Khattam and Salama, 2004; Khetrapal, 2020). While DG produces more energy to the available capacity, wheeling of the energy via the existing utility distribution network distorts the characteristics of the network. The voltage profile, thermal loading, line losses and fault level of the utility network could be affected by connection of DG for wheeling energy. The Gwarinpa Housing Estate (GHE) Abuja case study is powered through an existing 9-bus distribution network, and the characteristics of this 9-bus network could be distorted during energy wheeling from DG. For this reason, load flow analysis can be conducted to investigate the impact of energy wheeling from DG to the estate.

1.2 Problem Statement

A few years after the deregulation of the Nigerian power system, the major challenges faced by the consumers of electricity linger. The persistent trend of regulating power supply to consumers by the distribution companies is a major post-deregulation problem contributing to gross supply insufficiency to the consumers. The residential sector, being the dominant consumers, are the worst hit (Olaniyan *et al.*, 2018). Although consumers have long adopted self-generation from fossil fuel-powered generator sets and renewable sources such as photovoltaic systems, the option comes with an unbearable financial burden (Murray, 2018; Nemeth-Durko *et al.*, 2020; Olaniyan *et al.*, 2018).

The residential load case study, Gwarinpa Housing Estate (GHE), suffers from unstable electricity and supply deficit similar to other consumers. Only about half of the 60 MW capacity is available to the estate due to inadequate power generation and the transmission substation's transformer load capacity limitation. However, the estate stands out as the largest concentration of residential loads in Nigeria, with a population estimate of 178, 552 (Areo *et al.*, 2019). Thus, the estate is characterized by huge, diverse, stochastic and distinct residential load suitable for the research. . Globally, researchers have evaluated

the impact of grid-connected DGs and energy wheeling to industries regarded as economically critical, and results have shown prospects for improved and economical alternative electricity supply (Ayadi *et al.*, 2018; Azerefegn *et al.*, 2020; Dyak *et al.*, 2016; Krishnamoorthy *et al.*, 2020; Weng, 2016).

However, wheeling energy from renewable DG to residential electricity consumers using the distribution network leaves much to be desired and, thus, recommended (Murray and Adonis, 2019; Murray, 2018; Tukur and Solomon, 2019). Therefore, this research investigates the characteristics of the existing utility distribution network, with and without energy being wheeled from renewable DG to GHE. Thus, the impact of the DG on the voltage profile, fault level, line losses and thermal loading of the utility network was determined, and the concern on viability ascertained.

1.3 Aim and Objectives

This research aims to investigate the impact and viability of energy wheeling from renewable distributed generation to residential loads of Gwarinpa housing estate, Abuja, as an alternative approach to improved energy delivery.

The objectives are to;

i. Determine the optimum hybrid renewable energy potential for DG that meets the load demand of Gwarinpa housing estate, based on Levelized Cost of Energy (LCOE) and Net Present Cost (NPC) using HOMER.
ii. Model and simulate the GHE distribution network in DIgSILENT for load flow studies.

iii. Determine the impact and comparatively analyze the voltage profile, fault level, line losses and thermal loading of Gwarinpa housing estate's distribution network with and without renewable DG integration using DIgSILENT.

iv. Determine the viability of wheeling renewable DG to residential loads based on the outcome of objective iii.

1.4 Justification for the Research

Researchers have validated deregulation of power systems to attract investments that could improve electricity supply. This is evident in the fact that the Nigeria electricity supply industry (NESI) is undergoing a transformation with the provisions of EPSRA, 2005. There will be a paradigm shift from a centralized power generation to DG, as Independent Power Producers (IPP) take advantage of the deregulated system. Energy wheeling of DG would become imperative and widespread, providing an alternative means to improve supply and minimizes grid power deficit to consumers. Furthermore, the predominance of residential consumers in Nigeria and the diverse and stochastic characteristics of residential load make it necessary to evaluate the energy wheeling system to this category of consumers. Therefore, this research investigates the impact and viability of this system on the GHE Distribution Network.

1.5 Scope and Limitation

The scope of this research study is to determine the viability of wheeling renewable distributed energy to residential load by evaluating the impact assessment of the system. This research study will comparatively investigate the characteristics of the existing and the modified network (renewable DG-connected network). The mode of DG connection and synchronization technicalities was not considered. Furthermore, the work did not

cover the entire residential electricity-consuming population of Nigeria or the national grid but was limited to the selected residential estate and its power supply network.

CHAPTER TWO

2.0 LITERATURE REVIEW

This chapter presents a literature review on electricity consumption and distributed generation technologies with focus on solar photovoltaic system, wind energy system and the energy storage system. The chapter also provides a review of various optimization tools for carrying out a techno-economic assessment of renewable distributed generation and wheeling of energy. Lastly, related works were presented and discussed.

2.1 Electricity Consumption

Electricity is a major driving force for the development of any nation. The consumption of this important commodity is widely used as an index of economic development (Nemeth-Durko *et al.*, 2020). It is required for domestic and socio-economic activities by all facets of the global economy (Ezenugu *et al.*, 2017; Oyedepo, 2019). The Electricity consumption population, grouped into three sectors, consists of the residential, commercial and street lighting, and industrial sectors (Alao, 2016; Azodo, 2014). Comparatively, the residential sector accounts for about 30 % of total electricity consumption globally (Taale and Kyeremeh, 2019).

2.1.1 Global residential electricity consumption

Globally, one- third of final energy is consumed by the residential sector (Chen *et al.*, 2016; Nemeth-Durko *et al.*, 2020; Olaniyan *et al.*, 2018; Sachs *et al.*, 2019; Taale and Kyeremeh, 2019; Wang *et al.*, 2020). In developing countries such as Nigeria, the residential sector accounts for the largest consumption at 60 % (Alao, 2016; Babatunde and Shuaibu, 2009; Olaniyan *et al.*, 2018). Residential electricity consumption accounts for over 39 % of the total electricity consumption in Ghana (Diawuo *et al.*, 2019), 23 %

in South Africa (Bohlmann and Inglesi-Lotz, 2018), 50 % in Egypt (Nassar *et al.*, 2020) and 48.1 % in Saudi Arabia (Imam and Al-Turki, 2020). In more developed countries, the residential electricity consumption accounts less in the total electricity consumption due to higher industrial loads. It is 14.15 % in China (Wen and Yuan, 2020; Xin-gang and Pei-ling, 2020), 30 % in Britain (Ma *et al.*, 2020), 22 % in Turkey (Gugul and Koksal, 2017; Guo *et al.*, 2018), 27 % in HongKong (Durmaz *et al.*, 2020), 20 % in Netherlands (Kewo *et al.*, 2020), 17.6 % in Taiwan (Su, 2020), and so on. Socioeconomic parameters including per capita income, urbanization, population, electricity price and direct use of electricity are factors that affect residential electricity consumption (Chen, 2017; Diawuo *et al.*, 2019; Lin and Wang, 2020b; Nemeth-Durko *et al.*, 2020). Previous research work showed direct correlation between residential electricity consumption and the aforementioned socio-economic factors, as reported by (Diawuo *et al.*, 2019; Durmaz *et al.*, 2020; Guo *et al.*, 2018; Lin and Wang, 2020a; Lin and Zhu, 2020; Uzoh *et al.*; Xin-gang and Pei-ling, 2020). Similarly, previous research was carried out on the effect of direct use of household appliances on residential electricity consumption (Gugul and Koksal, 2017). Figure 2.1 shows graphical representation of the global residential electricity consumption.

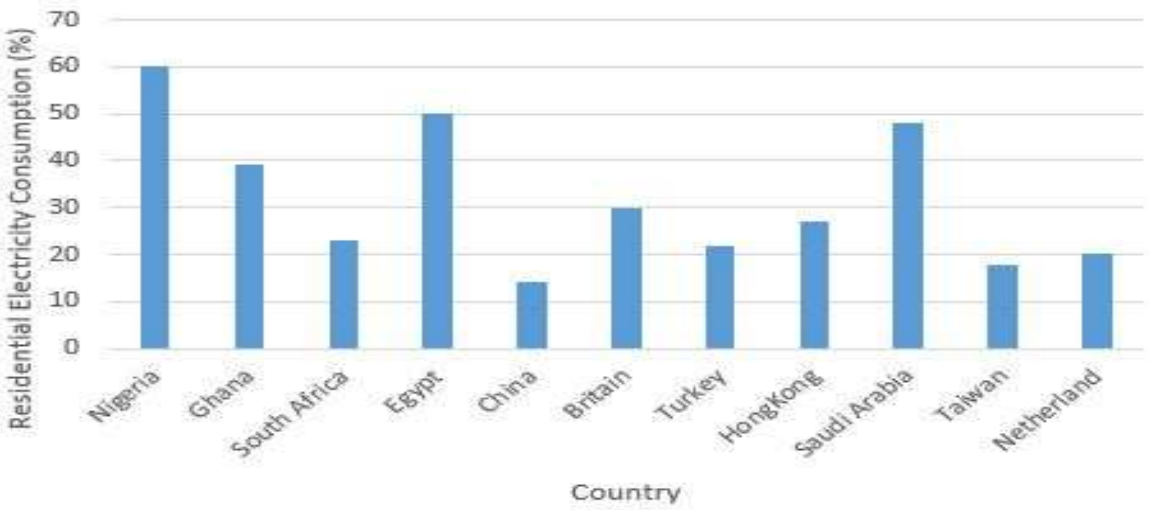

Figure 2.1: Global residential electricity consumption

2.1.2 Residential electricity consumption in Nigeria

The large informal sector, which makes a huge part of the Nigerian economy, where small and medium-scale enterprises were embedded within the residential electricity consumers, is a major contribution to the size of the residential electricity consuming population (Alao, 2016). The residential sector consumes about 60 % of the total electricity consumption in Nigeria (Babatunde and Shuaibu, 2009; Nwachukwu *et al.*, 2014; Olaniyan *et al.*, 2018). The residential sector of the Nigerian economy is characterized by huge population across the cities, towns and villages. Clusters of residential estates are a major component of the residential population. As the demand for electricity increases, access rate stood at 45% with electricity accounting for only 2% of the total final energy consumption (Momoh, 2019). The gap between demand and supply of electricity in Nigeria remain wide and contributes to incessant power outages to consumers, particularly the residential sector that consumes most of the power generated. It is estimated that about 60,000MW is required for stable power supply which could be achieved by substantial mix of renewable energy (Olaoye *et al.*, 2016).

2.2 Distributed Generation

The quest for improvement of power generation capacity to meet the ever increasing demand, brought about paradigm shift from the regulated, vertical integration model to deregulated system, led to the emergence of distributed generation (DG) (Infield and Freris, 2020). Distributed generation is the generation of electricity, usually small-scaled, at or near end users. DG technologies are of different types, and consists of the traditional (combustion engines) and non-traditional generators as shown in Figure 2.2 (El-Khattam and Salama, 2004). In the context of this research, focus is on the DG from renewable energy sources.

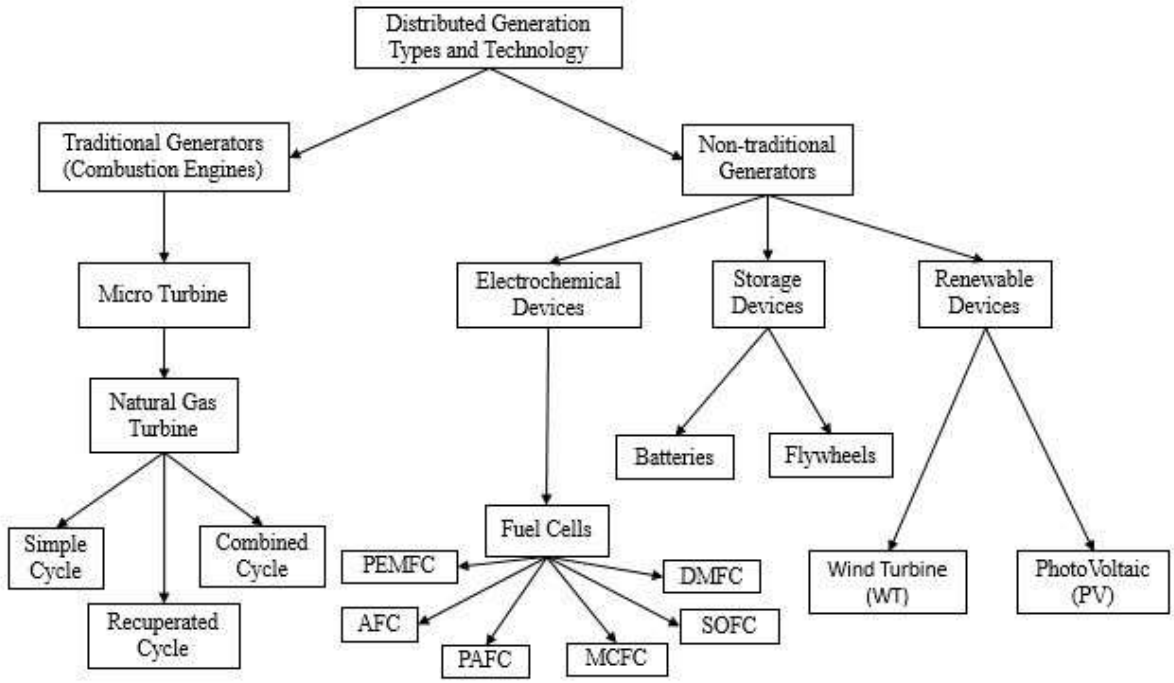

Figure 2.2: Distributed generation types and technologies (El-Khattam and Salama, 2004).

2.3 Distributed Generation from Renewable Energy Sources

Distributed generation from renewable energy refers to the generation of electricity from self-replenished sources and not earthly depleted (Owusu and Asumadu-Sarkodie, 2016). It is usually small-scale and low voltage with the point of connection close to the end users. However, connecting DG to the end-user distribution network poses challenges to the usual vertical system of power flow (Infield and Freris, 2020). While renewable energy sources are numerous, this research work is focused on solar and wind energies due to their abundance and ease of accessibility.

2.3.1 Solar energy resource

Sun provides the major source of renewable energy that is easily harnessed. On average, solar radiation intercepted on the earth's surface amounts to about 8000 times the size of the global primary energy consumption rate of 500EJ, equivalent to 1.4×10^{17}Wh (Infield

and Freris, 2020). In a day, about 120×10^5 Watts of solar energy, which falls on the earth's surface can meet the global energy demand for over 20 years (Ahmadi *et al.*, 2018). Solar energy is harnessed directly or indirectly with solar PV and concentrated solar power, respectively. For this study, solar PV is considered because of its applicability and sustainability to both high and low solar radiation, suitability for small to medium-scale generation and better electricity output in the specific sized area (Ahmadi *et al.*, 2018).

2.3.1.1 *Solar photovoltaic*

A photovoltaic (PV) cell, or solar cell, is a solid-state electrical device that converts solar radiation into electrical energy. The assemblage of PV cells, usually in a frame, forms the PV module, and interconnection of modules form a PV array (Al Momani *et al.*, 2017; Murray, 2018; Olatomiwa, 2016b). Figure 2.3 (a) and (b) show the schematic circuit diagram of solar cell supplying load and its working principle respectively (Cagnazzi, 2020).

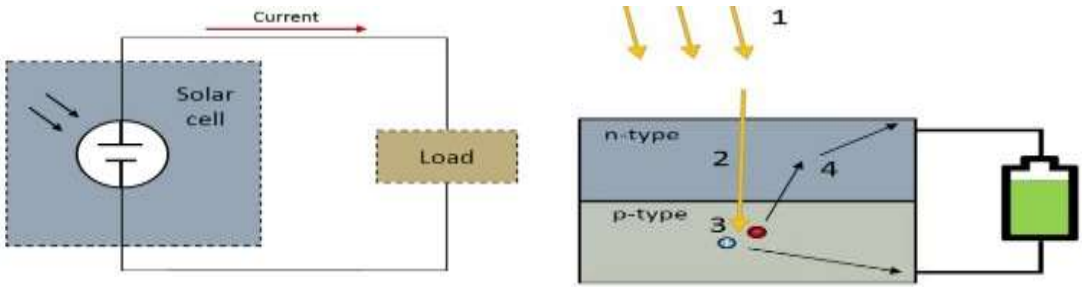

(a) Schematic circuit diagram of solar cell supplying the load.

(b) Schematic circuit diagram of the working principle of the solar cell.

Figure 2.3: Photovoltaic solar cells (Cagnazzi, 2020).

From Figure 2.3 (b), the surface of solar cells are bombarded by photons (denoted as 1) from solar radiation, taking their energy through the cell (marked as 2). The photon energy is transferred to electron producing electron/hole pair in the p-type, region as

indicated in point 3 of Figure 2.3(b). The energized electron flows into the n-type region (marked as point 4) and around the circuit to charge the battery.

The graph of I-V and P-V, shown below in Figure 2.4, represents the electrical characteristics of PV module.

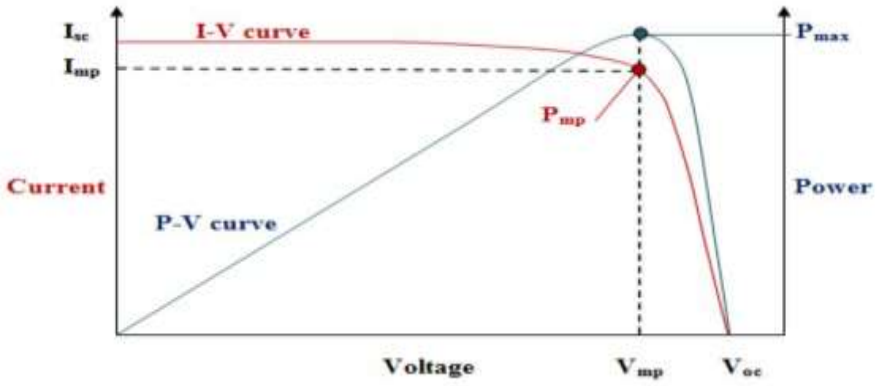

Figure 2.4: The I-V and P-V characteristic curves of PV module (Al Momani *et al.*, 2017).

PV modules are made of the following technologies:

i. Mono-crystalline silicon cells, Figure 2.5(a), belongs to first generation solar cells and most predominant. They are silicon wafers produced from a single homogenous crystal with up to 25 % cell efficiency for the p-type passivated emitter rear contact (p-PERC) (Kale *et al.*, 2019). These cells are characterized by high refractive index and optical reflection of up to 40 %, which can be minimized by surface texturization of the silicon wafers (Basher *et al.*, 2019).

ii. Poly-crystalline silicon cells, Figure 2.5(b), belongs to first generation solar cells. They are produced from molten silicon. The cells have lower conversion efficiency, typically between 13 to 15 % (Cagnazzi, 2020; Murray, 2018).

iii. Thin film solar cells, Figure 2.5(c), belongs to second generation solar cells. They are produced from deposits of photovoltaic material on a glass, plastic or metal

substrate. Examples of thin film solar cells include copper indium gallium selenide (CIGS), cadmium telluride (CdTe) and amorphous silicon. The thin film solar cells generally have lower conversion efficiency of 5-12 % (Cagnazzi, 2020; Murray, 2018). However, a record 14 %, 22.1 %, and 22.6 % for the amorphous, CdTe and CIGS types, respectively was reported in (Cagnazzi, 2020).

iv. Multiple junction cells are the third-generation solar cells, produced from layers of different photovoltaic materials deposited on one another to improve efficiency. This can yield 33 % theoretical cell efficiency (Murray, 2018).

v. Polymer solar cells also belong third-generation solar cells. They are not commercially abundant like the silicon solar cells. The cells are produced from organic material with performance of about 12 % attained. Polymer cells have the advantage of flexibility, low cost of material and can be coated or printed from a solution. In polymer solar cells, a conjugated polymer with semiconductor characteristics is used to absorb solar radiation (Cagnazzi, 2020). This is shown in Figure 2.6

vi. Perovskite solar cell is also a type of thin film solar cell under research. The cell has shown potential with record efficiency above 20 % over a very small area (Cagnazzi, 2020).

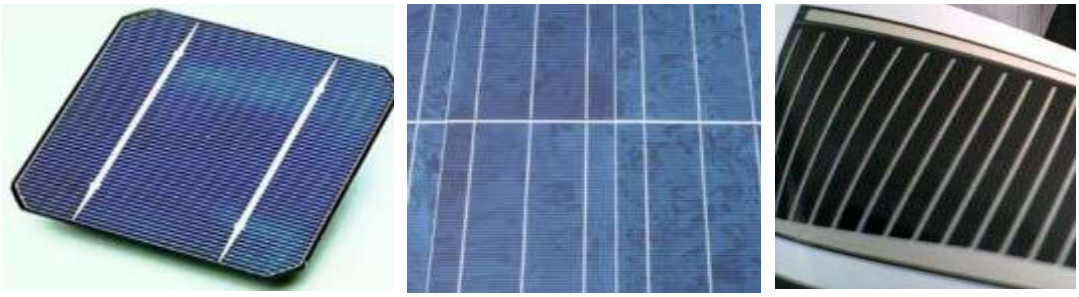

(a) Monocrystalline silicon module

(b) Polycrystalline silicon module

(c) Thin film solar module

Figure 2.5: PV module technologies (Cagnazzi, 2020).

Figure 2.6: Polymer solar cells (Cagnazzi, 2020).

2.3.1.2 *Photovoltaic systems*

PV systems are generally classified into stand-alone and grid-connected.

i. Stand-alone PV systems

As the name connotes, stand-alone PV systems are designed to operate without connection to the grid. The system supplies DC directly to the DC load or to AC load via the application of DC/AC inverter. This system has wide application for residential and commercial supply. The stand-alone system can be designed along with one or more other sources, such as wind, generator set and so on, to produce a hybrid system.

ii. Grid connected PV systems

The grid-connected system is designed and interconnected with the utility system. The main components are the inverter for conversion of DC output of the PV systems to AC power, step up transformer for producing the required voltage level, a bi-directional AC interface between the PV system AC output and the grid network for power flow regulation (Cagnazzi, 2020).

2.3.1.3 *Solar photovoltaic performance*

According to the provisions of International Energy Agency (IEA), the performance of PV systems are measured based on the following IEC 61724 parameters (Marion *et al.*, 2005):

i. Final yield: This parameter defines the energy production of the PV system and is dependent on the hours of the same energy production at rated power of the PV. The final yield is expressed as:

$$Y_f = \frac{E_n}{P_{d.c}} \tag{2.1}$$

Where Y_f is the final yield of the PV measured in kWh/kWp or in hours. E_n is the output net energy and $P_{d.c}$ is the output D.C power on the nameplate of the PV system.

ii. Reference yield: This parameter determines the PV solar radiation resource based on location, weather and PV orientation.

$$Y_r = \frac{G_i}{G_r} \tag{2.2}$$

Where $Y_{r.}$ is the reference yield measured in hours, G_i and G_r are the total in-plane and reference irradiance respectively.

iii. Performance Ratio: The performance ratio determines the effect of total system losses on the output and is expressed as:

$$R_P = \frac{Y_f}{Y_r} \tag{2.3}$$

Where performance ratio is denoted as R_P. The PV temperature, inefficiency of inverter, loss of incident irradiance on PV surface, conversion of D.C to A.C, wiring, and weather contributes to the overall system losses.

2.3.1.4 *Solar photovoltaic potential in Nigeria*

Due to its geographical location, Nigeria has enormous solar energy potential. It is one of the most explored renewable energy resources due to its abundance and ease of accessibility (Infield and Freris, 2020; Olatomiwa, 2016a). Nigeria is divided into three solar radiation zones (Adaramola, 2014). The North-East classified as zone I, has potential for large-scale power generation. The zone is characterized by long sunshine hours, about 6 hours per day, with solar radiation of 5.7–6.5 kW/m2/day. The North-West and Central as zone II, also has great potential for solar power. The zone has about 5.5 hours per day of sunshine and solar radiation of 5.0–5.7 kW/m2/day. While zone III of the Southern Nigeria has lower potential, though viable for decentralized and stand-alone applications. The zone has about 5 hours per day of sunshine with 3.5–5.0 kW/m2/day (Adaramola, 2014). Figure 2.7 shows the solar radiation map of Nigeria (Adaramola, 2014). This research is focused on zone II and Abuja specifically, where the residential area of the study lies. Abuja has an estimated monthly global solar radiation ranging between 129.9 kWh/m^2 to 194.4 kWh/m^2 and annual global solar radiation of 1988.8 kWh/m^2 (Agbetuyi *et al.*, 2018).

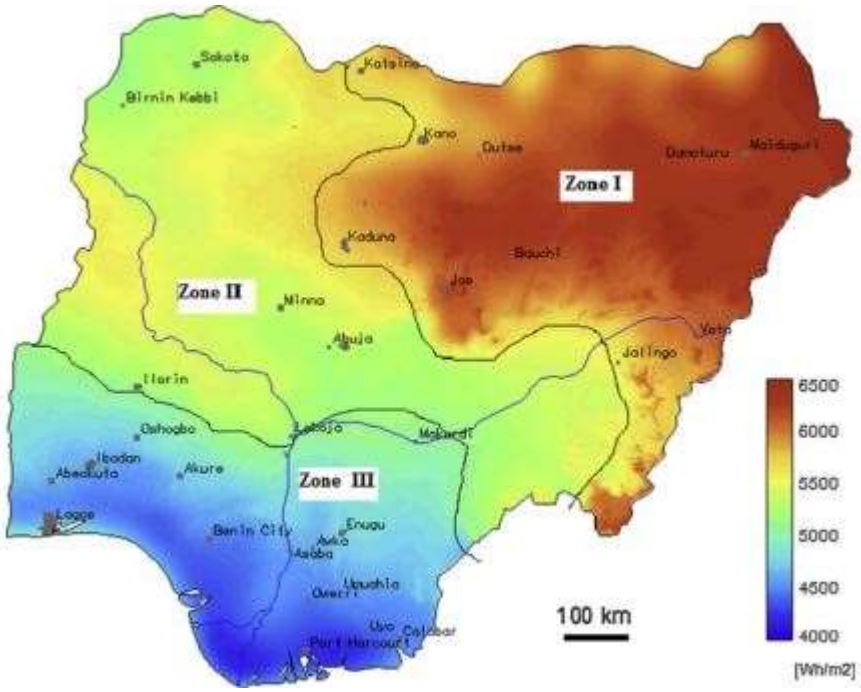

Figure 2.7: Solar radiation map of Nigeria (Adaramola, 2014).

2.3.2 Wind energy resource

Wind energy is also an abundant renewable energy source for electricity production. It involves the conversion of the wind's kinetic energy into electrical energy. This source of electrical energy is clean and environmentally friendly, cheap, easily harnessed, sustainable and inexhaustible (Ahmed and Kunya, 2019; Ajayi *et al.*, 2014; Ayodele and Ogunjuyigbe, 2015; Ayodele *et al.*, 2018; Bhutta *et al.*, 2012; Owoeye *et al.*, 2017; Tummala *et al.*, 2016).

2.3.2.1 *Wind energy systems*

The wind energy technology is basically the wind turbine. The turbine is made of the blades, generator, gearbox and other associated parts, as shown in Figure 2.8. The wind turbine can be likened to fan blades, but in the opposite mode of operation. While fan produces 'wind' from electricity, the wind turbine produces electricity from the wind.

The wind from the atmosphere turns the blades connected to the rotor, which energizes the generator to produce electricity (Annapolis, 2020).

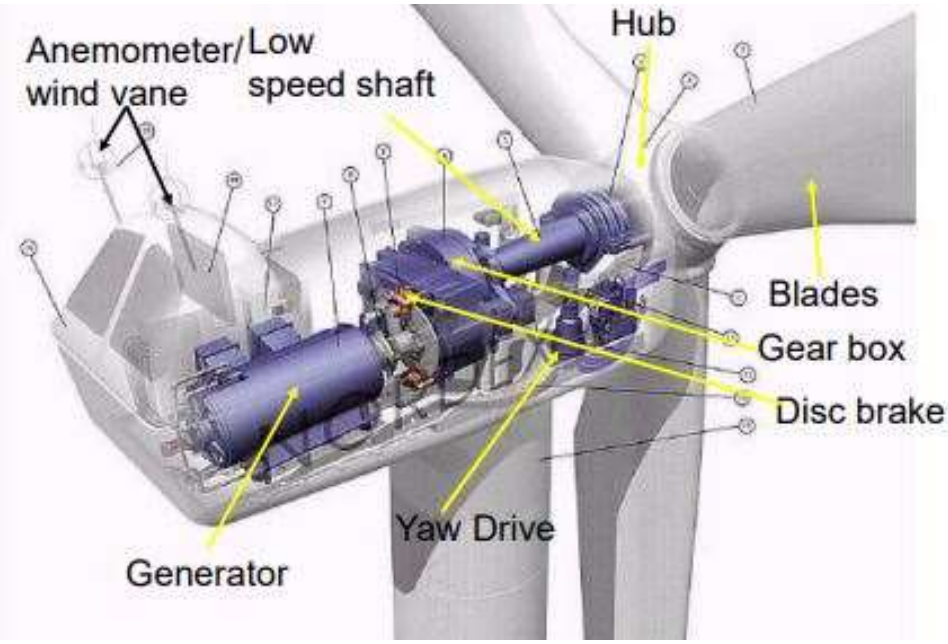

Figure 2.8: The parts of a wind turbine (Annapolis, 2020).

The turbines are generally classified into two types based on axis of rotation. The Horizontal Axis Wind Turbine (HAWT) and the Vertical Axis Wind Turbine (VAWT) (Ahmed and Gawad, 2016; Annapolis, 2020; Ayodele and Ogunjuyigbe, 2015; Bhutta *et al.*, 2012; Tummala *et al.*, 2016). The former is predominantly used due to higher efficiency and lower cost to power ratio over the latter (Johari *et al.*, 2018; Marinić-Kragić *et al.*, 2019). However, wind turbines are also classified based on rotor diameter, power rating, and aerodynamic force (Johari *et al.*, 2018; Kumar *et al.*, 2018; Tummala *et al.*, 2016) as shown in Figure 2.9.

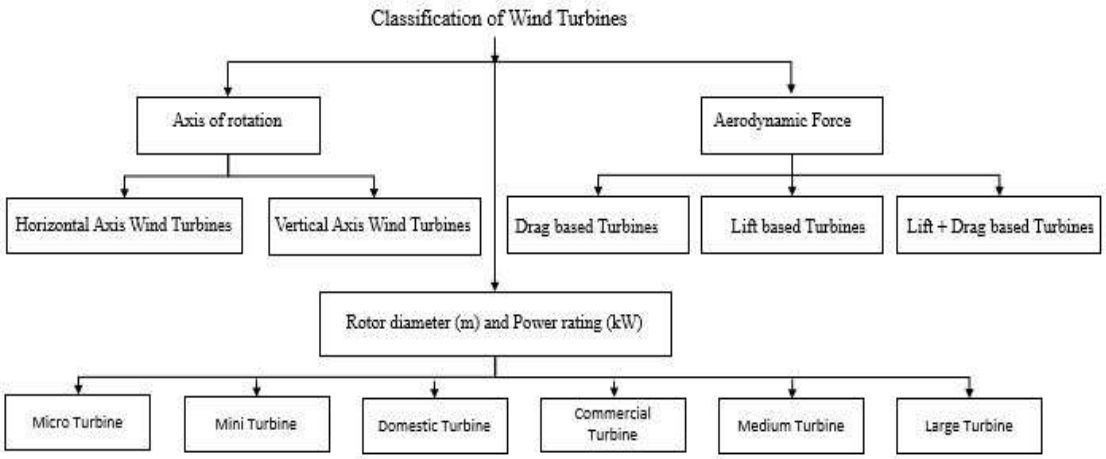

Figure 2.9: Classification of wind turbines (Kumar *et al.*, 2018).

The HAWT consists of the tower, the blades and the nacelle which contains the gearbox, generator, transformer and other components of the turbine structure. VAWT, on the other hand, is less complex in design, produces less noise and is suitable for small-scale applications (Marinić-Kragić *et al.*, 2019). Figure 2.10 shows the schematic structure of the HAWT and the VAWT (Ayodele and Ogunjuyigbe, 2015).

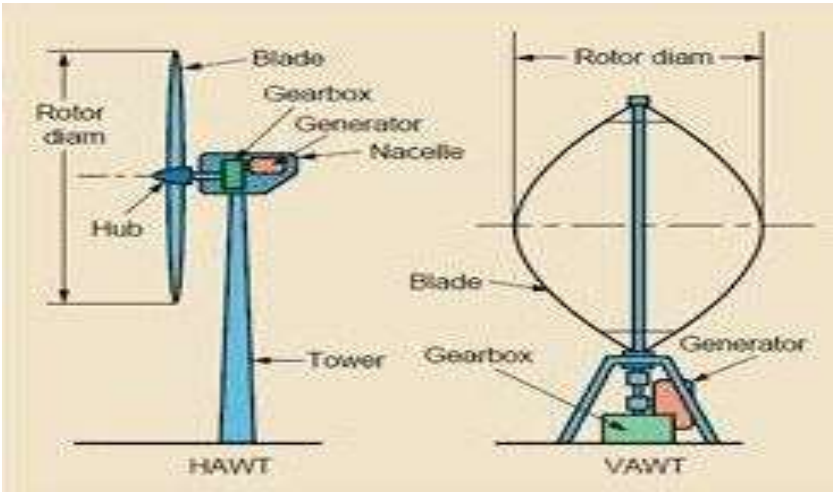

Figure 2.10: The schematic diagram of horizontal and vertical axis wind turbines (Ayodele and Ogunjuyigbe, 2015).

2.3.2.2 *Wind turbine performance*

The performance of a wind turbine is affected by three basic parameters. These are the power curve, hub height and distribution of wind speed at a particular area (Olatomiwa, 2016b).

1. Power Curve: At a given wind speed, the power output power of a wind turbine is obtained from the power curve provided by the manufacturer (Olatomiwa, 2016b).
2. Wind speed distribution: This is usually obtained using the Weibull distribution function expressed as:

$$F(v,k,c) = \frac{k}{c}\left(\frac{v}{c}\right)^{k-1} \exp\left[-\left(\frac{v}{c}\right)^{k}\right] \tag{2.4}$$

And the cumulative probability function is:

$$F(v,k,c) = 1 - \exp\left[-\left(\frac{v}{c}\right)^{k}\right] \tag{2.5}$$

Where; $v \geq 0$, $k > 1$, and $c > 0$ and v, k, c are the wind speed, scale and shape parameters respectively.

3. Turbine hub height: The power law, among numerous expressions of the wind speed and hub height, provides a simplified relationship given as:

$$\frac{v}{v_0} = \left(\frac{h}{h_0}\right)^{\alpha} \tag{2.6}$$

Where v is the velocity of the wind at a desired height of the hub, h. while v_0, h_0 are the velocity at reference height and α is the coefficient for surface roughness of a given area.

2.3.2.3 *Wind energy potential in Nigeria*

Nigeria has great wind energy potential for electricity generation. The far northern region has wind speed ranging from approximate values of 4.0 m/s to 5.12 m/s, with annual average of between 2m/s to 4 m/s at hub heights of 10 m. The Southern region has lower potential, with wind speed between 1.4 m/s to 3.0 m/s. Studies have shown high wind energy reserve that could be harnessed to produce 97 MWh/year in Sokoto and 51 MWh/year in Jos (Ahmed and Kunya, 2019; Aika *et al.*, 2020; Ayodele *et al.*, 2018; Olanipekun and Adelakun, 2020; Olomiyesan *et al.*, 2017). Abuja, North Central Nigeria, being the location of focus for this research work, has an annual mean wind speed of 3.244 m/s at hub height of 10 m (Owoeye *et al.*, 2017). Figure 2.11 and 2.12 shows the wind speed and wind farm suitability map of Nigeria respectively (Ayodele *et al.*, 2018).

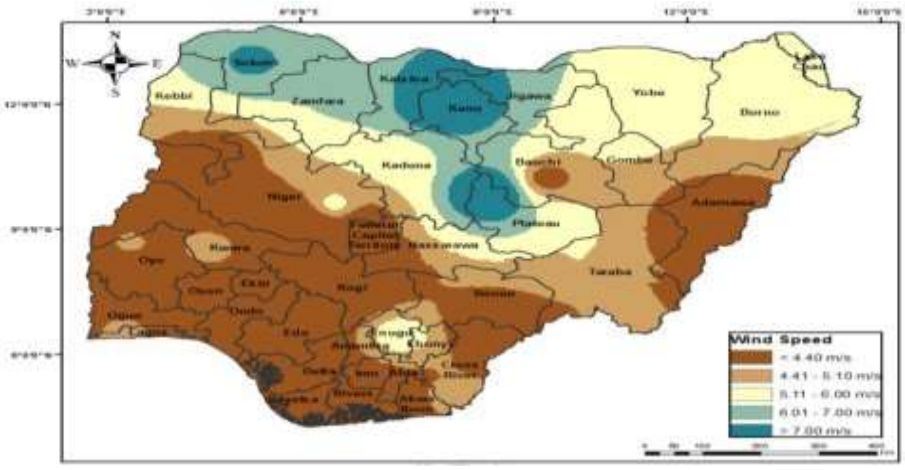

Figure 2.11: The wind speed map of Nigeria (Ayodele *et al.*, 2018).

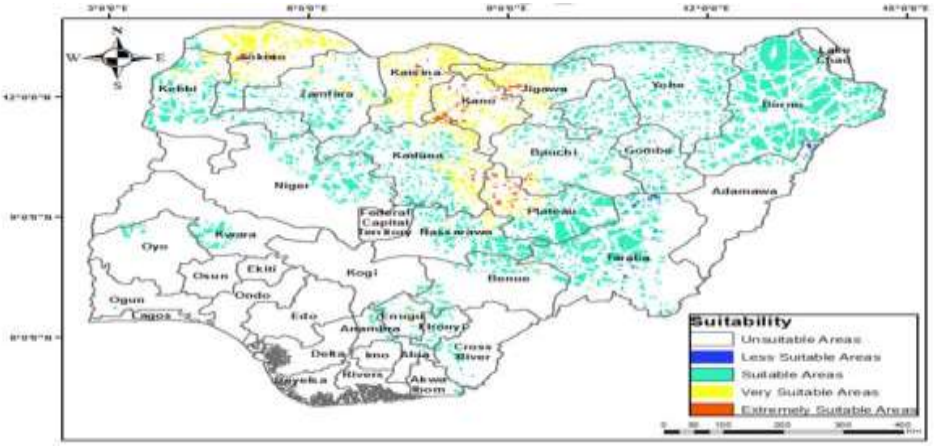

Figure 2.12: Wind farm suitability map of Nigeria (Ayodele *et al.*, 2018).

2.3.3 Energy storage systems

One major problem associated with renewable energy resources is intermittency due to weather and climatic conditions (Barzegkar-Ntovom *et al.*, 2020; Olatomiwa *et al.*, 2015). The energy storage systems provides the means of storing electrical energy that could be made available when the renewable resources are unavailable. Thus, the energy storage systems ensures efficient utilization of the renewable energy resources, which enhances power system reliability and security (Kucevic *et al.*, 2020; Olatomiwa *et al.*, 2015; Yang *et al.*, 2018).

Energy storage methods in power systems include the following; thermal storage system, electro-chemical storage system (battery storage), electro-mechanical storage system and pumped hydro storage system with a global installed capacity of 169 GW, equivalent to 96 % (Murray, 2018). Battery storage accounts for approximately 2GW, 1.1 % of the total installed capacity. Figure 2.13 shows the global installed capacity of the energy storage systems according to the International Renewable Energy Agency (IRENA), 2017.

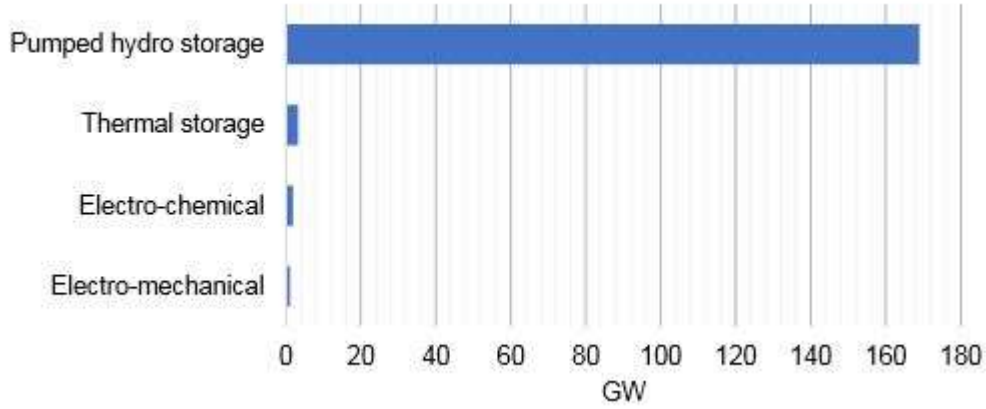

Figure 2.13: Global capacity of stationary energy storage (Murray, 2018).

2.3.3.1 *Battery energy storage systems (BESS) and technologies*

With a global installed capacity of about 10 GWh, IRENA, 2017 (Figgener *et al.*, 2020), the application of BESS has witnessed significant growth due to increased deployment of renewable energy systems, technological advancement, reduced cost and provision of ancillary services (Barzegkar-Ntovom *et al.*, 2020; Figgener *et al.*, 2020; Mexis and Todeschini, 2020). The integration of BESS components in PV systems enhances residential energy utilization and sufficiency (Barzegkar-Ntovom *et al.*, 2020). Battery technologies includes the lithium-ion batteries, lead-acid batteries, alkaline batteries and the silver batteries. Though both the lithium-ion and the lead-acid batteries are the commonest in existence (Murray, 2018), the lead-acid is more often used in hybrid renewable energy systems (Olatomiwa *et al.*, 2015). Figure 2.14 shows the capacities of battery energy technologies according to IRENA 2017

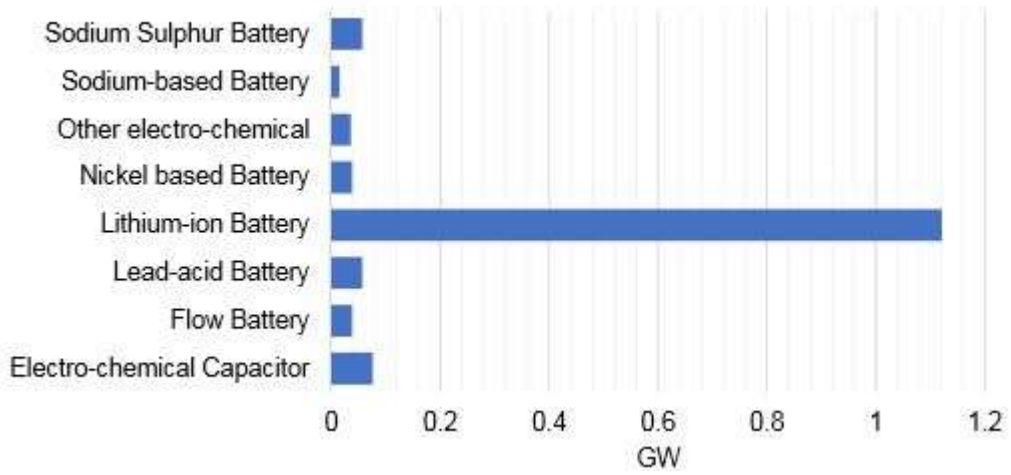

Figure 2.14: Capacities of battery energy technologies, IRENA 2017 (Murray, 2018).

The battery capacity, at any time t, depends on certain factors, including the previous state of charge (SOC), availability of energy from the source components, and the load demand.

2.3.4 Hybrid renewable energy systems (HRES)

The integration of two or more single renewable energy system discussed above, forms the hybrid renewable energy system (Kumari *et al.*, 2017; Olatomiwa, 2016b). The cluster of the renewable energy components that produces the HRES, operates independently but in a well-coordinated manner (Olatomiwa *et al.*, 2015; Olatomiwa, 2016b). The HRES minimizes the effect of intermittency, ensures sustainability and higher reliability of supply over the single energy systems (Bilal *et al.*, 2016; Kalappan *et al.*, 2020; Krishnamoorthy *et al.*, 2020; Lipu *et al.*, 2017; Olatomiwa *et al.*, 2018). There are various possible HRES including but not limited to the following; Solar-Wind-Battery system, Solar-Wind-Battery-Grid system, Solar-Wind-Grid. A typical HRES configuration is shown in Figure 2.15 (Mercado *et al.*, 2016).

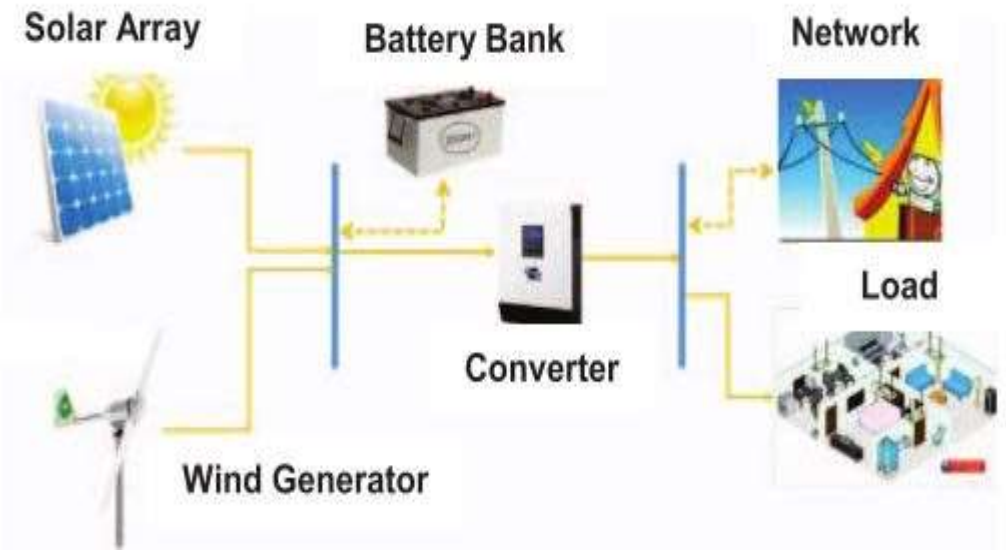

Figure 2.15: Hybrid renewable energy system configuration (Mercado *et al.*, 2016).

2.3.5 Optimum system configuration

This is required to meet the system load demand. This is achieved by conducting the power system reliability and the system life-cycle cost analysis.

i. Power system reliability analysis:

This aims at designing the most economical and cost-effective system that meets the load demand. Methods used include Loss of Load Probability (LOLP), which is a probability measure of the system demand exceeding supply capacity of the system at a given time. The Loss of Power Supply Probability (LPSP), is a measure of the system probability of supply inadequacy due to the inability of the hybrid system supply to meet the load demand. The Loss of Load Hours (LOLH) is associated with LOLP. It's a measure of the hours load exceeds supply in a year. The System Performance Level (SPL) measures the probability that load demand cannot be met (Negi and Mathew, 2014).

ii. System life-cycle cost analysis

This analysis includes the Net Present Cost (NPC) which has 3 components; the initial cost of components, the cost of replacement and the cost of maintenance. The Levelized

Cost of Energy (LCOE) is a ratio of the total cost of the system per annum to the annual electricity supplied by the system (Negi and Mathew, 2014). NPC and LCOE are expressed in Equations (2.7) and (2.8), respectively.

$$NPC = \sum_{t=1}^{n} \frac{c_t}{(1+r)^t} \tag{2.7}$$

Where c_t is the cost per annum for t years, n is the project lifetime in years and r, the annual discount rate.

$$LCOE = \left(\frac{c_e - c_b h_s}{e_s} \right) \tag{2.8}$$

where c_e is the annual cost of electricity produced, c_b is the total marginal boiler cost, h_s and e_s are the total heat and total electricity served respectively.

2.3.6 Optimization techniques and software packages

To mitigate the challenges associated with HRES generation, such as the impact on system voltage profile, power losses, loading and faults. Several optimization techniques have been used to conduct techno-economic evaluation to design hybrid systems. These include the Hybrid Optimization for Multiple Energy Resources (HOMER), Hybrid Optimization by Genetic Algorithm (HOGA), Integrated Simulation Environment Language (INSEL), Transient System (TRNSYS), Photovoltaic systems (PVsyst), Digital Simulation of Electrical Networks (DIgSILENT) and so on. For this research work, HOMER and DIgSILENT software were chosen to conduct the techno-economic assessment.

2.3.6.1 *Hybrid optimization for multiple energy resources* (HOMER)

The HOMER software, a product of the National Renewable Energy Laboratory (NREL) of the United States of America, is a renewable energy-based, general purpose system design and optimization tool(Olatomiwa *et al.*, 2015) with the capability to simulate, optimize and performs sensitivity analysis of different hybrid scenarios to determine the optimal configuration for both off-grid and grid integrated systems and avail users the accessibility of techno-economic feasibility outcomes (Akinyele, 2017; Al Ghaithi *et al.*, 2017; Olatomiwa and Blanchard, 2019). HOMER performs simulation process modelling of hybrid configuration based on each time step. The optimization process considers various scenarios to determine the configuration that fulfills system constraint at the minimum life-cycle cost (Magarappanavar and Koti, 2016). HOMER also conducts Sensitivity analysis that involves performing different optimizations to determine the techno-economic impacts on the optimized system configurations. Several inputs, such as the load demand data, energy resources data, technologies and cost, are required for the optimization. HOMER makes a comparative analysis of the energy generated by different configurations with the load profile, every hour for the year. The NPC, operating cost and the LCOE optimal configuration that meets the load demand is then computed (Kumar and Deokar, 2018; Lipu *et al.*, 2017; Olatomiwa *et al.*, 2015; Radzi *et al.*, 2019).

2.3.6.2 *Digital simulation of Electrical network* (DIgSILENT)

DIgSILENT PowerFactory is a power system simulation software used for power system generation, transmission, and distribution applications. The software combines classical power system analysis such as voltage rise/drop calculation, unbalanced systems evaluation, fault level determination and so on, with modern power system tools such as quasi-dynamic simulations, and load flow probabilistic calculation. The software

conducts power system modelling, simulation and analysis. DigSilent tool creates system designs on a textual database environment with all power system components. DigSilent program offers various evaluation methods, such as Newton Raphson's method for balanced and unbalanced AC systems, and the linear DC method (Nassar *et al.*, 2020). The software is useful for both transient faults, such as grid faults and non-transient faults associated with power quality and control problems of wheeling energy (Hansen *et al.*, 2003).

2.4 Energy Wheeling

Energy wheeling refers to an intermediate, third-party transportation of electric energy from the producer to the consumer based on bilateral transaction agreement (Ramanathan, 2019; Saxena *et al.*, 2016). Wheeling is broadly divided into own use and not own use systems. In the own-use system, both the producer and the consumer, at a separate location, belong to a single entity. For not own-use system, the consumer is not owned by the producer (Santosa and Rusdiansyah, 2018). Wheeling transaction has cost of energy and cost of transmission. The charges are computed with several methodologies (based on techno-economic factors) such as MW-Mile, path-contract, post-stage stamp and marginal cost (Li *et al.*, 2017).

2.4.1 Energy wheeling charges

The use of the existing utility network attracts certain charges payable by the users, such as the IPP. Several methodologies have been adopted for calculating wheeling charges, some of which are (Lee *et al.*, 2001; Murray, 2018):

i. Contract Path: This method is based on a specified path of electricity flow within the wheeling utility transmission network. The cost of wheeling power along this

path is paid by the buyer. However, the buyer is not liable for power flow outside the specified path.

ii. Postage Stamp: This method is based on the assumption that the entire utility transmission network is involved in energy wheeling rather than actual wheeling path. This system has no regard for distance between the supplier and the buyer.

iii. Distance-based method: This method takes into cognizance the straight line distance between the producers and the buyers.

iv. Load flow-distance based: This method calculate the cost/megawatt-kilometer of the transmission line based on load flow.

v. Nodal pricing method: The cost are based on the nodal points.

Distributed generation predominantly from renewable energy sources, deployed for wheeling systems are known to create techno-economic imbalance that has been studied by several researchers (Infield and Freris, 2020; Sood *et al.*, 2002). Some of the distribution network indices are presented.

2.5 Distribution Network Performance Indices

The distribution network is designed to operate under certain conditions efficiently. The voltage profile, fault level, power losses and thermal loading are some of the critical characteristics of the system that are desired to be kept within designed limitations. These have been considered for this study, and presented.

2.5.1 Distribution network voltage profile

Voltage drop occurs between the source and the load and as the distance increases, voltage drop becomes significant (Murray and Adonis, 2019; Murray, 2018). The line impedance and the quantity of load current accounts for the loss. The grid code for the Nigeria power

system provides an operating range of 0.95p.u (10.45 kV) and 1.05p.u (11.55 kV) for 11 kV voltage level, 0.94p.u (31 kV) and 1.06p.u (34.98 kV) for 33 kV voltage level. Figure 2.16 shows a two-bus distribution network used for the illustration of voltage drop in distribution systems.

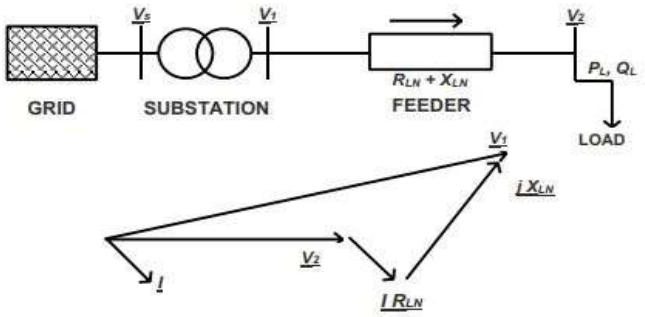

Figure 2.16: Voltage drop in a two-bus distribution network (Murray, 2018)

The current $\underline{I}$ is given by the Equation (2.9):

$$I = \frac{S}{V_2} = \frac{P_L - jQ_L}{V_2^*} \tag{2.9}$$

where $\underline{S}$ is the apparent power at the load bus 2, with voltage $\underline{V_2}$ conjugate, V_S is the transformer primary voltage (V), V_1 is the transformer secondary voltage (V), V_2 is the load bus voltage (V), P is the active power flow (W), Q is the reactive power flow (var), P_L is the active power at the load (W), and Q_L is the reactive power at the load (var).

The drop in voltage is given by,

$$V_1 - V_2 = I\left(R_{LN} + jX_{LN}\right) = \left(\frac{P_L - jQ_L}{V_2^*}\right)\left(R_{LN} + jX_{LN}\right) \tag{2.10}$$

The voltage angle $V_1 - V_2$ is small, for small voltage flow. Thus, the imaginary part of Equation (2.10) can be neglected. Therefore, the voltage drop becomes:

$$\Delta V \approx \frac{R_{LN} P_L + X_{LN} Q_L}{V_2^*} \tag{2.11}$$

Hence, from Equation (2.11), the voltage drop along a line is a function of P_L, Q_L, and most importantly V_2* which is obtained from load flow studies.

2.5.2 Distribution network fault level

Faults in power systems could be caused by equipment failure, maloperation, and natural phenomena such as thunder, tornadoes, etc. The equivalent voltage source is used to illustrate three-phase symmetrical short circuit as shown in Figure 2.17 (Murray, 2018).

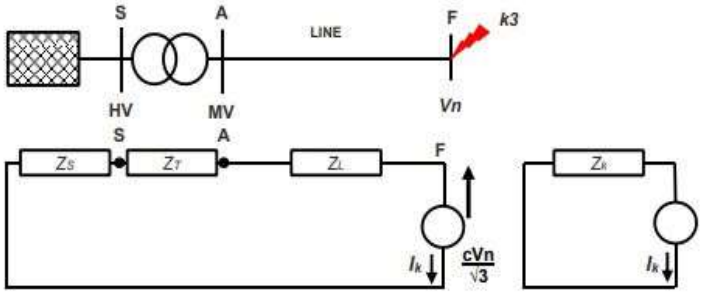

Figure 2.17: The symmetrical short circuit current using equivalent voltage source (Murray, 2018).

Using the equivalent voltage source, the three-phase symmetrical short circuit current is given as:

$$I_K = \frac{cVn}{\sqrt{3Z_K}} = \frac{cVn}{\sqrt{3}(Z_T + Z_L + Z_S)} \tag{2.12}$$

where Z_K is the equivalent short circuit impedance of the network at the fault location (Ω), Z_S = network impedance (Ω), Z_T = transformer impedance (Ω) and Z_L = load impedance (Ω) and *cVn* = equivalent voltage source with voltage factor c, for scaling equivalent voltage source in the calculations to account for system voltage variations.

2.5.3 Distribution network line losses

Line losses are a function of the line resistance and the magnitude of current flowing in the circuit.

The line losses in a distribution network is given by Equation (2.13) (Murray, 2018):

$$P_{loss} = 3 \times I_L^2 \times R \times L \tag{2.13}$$

where P_{loss} is the line losses (W), R is the line resistance (Ω), L is the substation to load distance in km, I_L is the line current (A).

2.5.4 Distribution network thermal loading

Power system equipment are designed to operate under certain specification such as the current carrying capability. Beyond the design limit, equipment may be overloaded, leading to excessive temperature rise and eventual insulation breakdown. Integrating DG provides additional capacity to relief overload.

2.6 Impact of Distributed Generation on Distribution Network Performance

For wheeling energy generated from DG sites of IPP, the integration of distributed generation to the existing distribution network is required. This operation alter the flow of power and could distort the network voltage profile, fault level, losses, and thermal loading (Khetrapal, 2020; Murray, 2018; Zhang and Zhu, 2021).

i. Voltage Profile

The voltage drop of a DG-connected distribution line is a function of the line voltage drop and the connected DG. It is required that integration of DG does not affect the network

beyond the allowable designed limits. The two-bus distribution feeder of Figure 2.16 is connected with DG as shown in Figure 2.18.

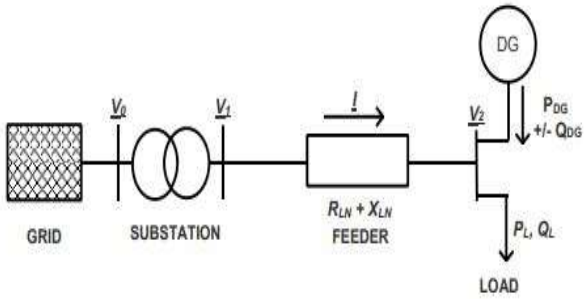

Figure 2.18: The DG-connected two-bus distribution line (Murray, 2018).

The voltage drop is expressed by Equation (2.14):

$$\Delta V = V_1 - V_2 \approx R_{LN}(P_L - P_{DG}) + X_{LN}(Q_L - (\pm Q_{DG})/V_2 \tag{2.14}$$

where P_{DG} is the active power generated by the DG and Q_{DG} is the reactive power generated by the DG.

ii. Fault Level

The integration of DG contributes to the system fault level, depending on the type, size, mode of connection and fault distance. The network of Figure 2.17 is connected with a DG, as shown in Figure 2.19, to determine the impact on fault level.

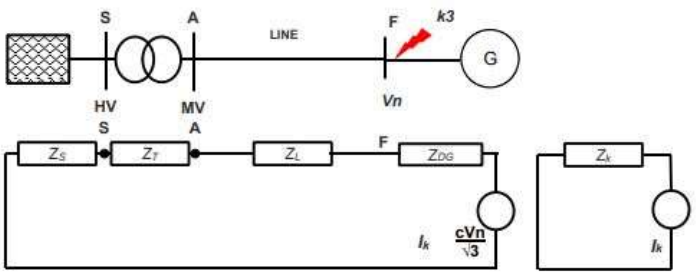

Figure 2.19: The symmetrical short circuit current of DG connected network using equivalent voltage source (Murray, 2018).

The short circuit current is expressed as:

$$I_K = \frac{cVn}{\sqrt{3Z_K}} = \frac{cVn}{\sqrt{3}(Z_S + Z_T + Z_L + Z_{DG})} \quad (2.15)$$

where Z_{DG} = equivalent impedance of the DG (Ω).

iii. Line Losses

With DG connected to the network, the total network losses is the sum of network losses between the substation and DG, and network losses between the load and DG (Murray, 2018).

The losses between the substation and DG is given as follows:

$$P_{loss(SDG)} = \frac{R \times G}{3V_L^2}(P_L^2 + Q_L^2 + P_G^2 + Q_G^2 + 2P_L P_G - 2Q_L Q_G) \quad (2.16)$$

And the losses between the load and DG are expressed as:

$$P_{loss(LDG)} = \frac{R \times L}{3V_L^2} = \left[(P_L^2 + Q_L^2) + (P_G^2 + Q_G^2 - 2P_L P_G - 2Q_L Q_G)\left(\frac{G}{L}\right) \right] \quad (2.17)$$

Therefore, the total network losses is expressed as:

$$P_{Tloss} = \frac{R \times (P_L^2 + Q_L^2)}{3V_L^2}(L - G) \quad (2.18)$$

where P_L is the active power of load (W), P_G is the active power of DG (W), Q_L is the reactive power of load (var), Q_G is the reactive power of DG (var), V_L is the load voltage (V), G is the distance between substation and DG (km), L is the distance between load and DG (km).

iv. Thermal Loading

Power system equipment are designed to operate under certain specification such as the current carrying capability. The transformers, cables, overhead line conductors and so on, efficiently operate within this limitation. Beyond the design limit, equipment may be overloaded, and this could lead to excessive rise in temperature and eventual breakdown of insulation. However, Integrating DG provides additional capacity that could relief overload. The thermal loading of a line can be expressed in current, active power flow and apparent power flow.

Hence, between 2-nodes/buses, the current flow measuring thermal loading is expressed by Equation (2.19):

$$I_T = \frac{V_i - V_j}{Z_{ij}} = V_i - V_j Y_{ij} \tag{2.19}$$

$$S = VI_T^*$$
$$\therefore S_{Ti} = V_i I_T^* = \frac{V_i(V_i - V_j)}{Z_{ij}} \tag{2.20}$$

where I and S are the current flow and apparent power flow respectively.

Distributed generation predominantly from renewable energy sources, deployed for wheeling systems are known to create techno-economic imbalance that several researchers have studied. The distribution network voltage, fault level, thermal loading, and line losses are some system characteristics subjected to distortion. The effort by researchers to investigate the impact of DG on distribution network characteristics is presented below.

2.7 Review of Related Works

The continued exploration of renewable energy resources for power generation has significantly improved supply to consumers. However, the utilization of renewable energy, particularly through integration to the existing power system network, are associated with certain challenges. Renewable energy fraction, intermittency, stability, impact assessment and so on have been the subject of several researches. Some of the research that relates to this work is therefore presented.

Murray (2018), carried out techno-economic analysis of a distribution network that supplies two industrial loads in South Africa and a comparison was made with a network powered by a DG using HOMER and DIgSILENT PowerFactory simulation software. DIgSILENT PowerFactory was used to assess the impact of DG technology and size on system parameters like voltage profile, line losses, fault level and equipment thermal loading. HOMER was used to evaluate cost analysis of wind, solar and hydropower energy.

The result showed solar and wind resources with greater potential having Global Horizontal Irradiance (GHI) level above 2200 kWh/m^2 and wind speed of 8 m/s at 100 m above sea level respectively. Furthermore, for both cases, wind energy was financially more viable with levelized cost of electricity (LCOE) at 0.065 $/kWh for 16 MW and 0.063 $/kWh for 70 MW. The impact of voltage profile was negligible on the buses, but was against the upper limit of 1.095pu as the distance between the DG and substation increases. The result also showed that the larger the size of DG, the higher is the fault contribution to the system. Distance affected both line losses and equipment thermal loading. Power loss became pronounced with increased distance between the load and the

DG. DG produced marginal increase in the thermal loading of the lines but dampened as it get farther from the load.

From the techno-economic analysis, the result showed realistic potential for wheeling of energy, particularly from the wind resources to large industrial loads (Murray, 2018). However, the study was limited to industrial load and the viability on residential load of diverse and stochastic characteristics was not examined.

A techno-economic assessment of an off-grid hybrid energy system was conducted in Masirah Island, Oman (Al Ghaithi *et al.*, 2017). Different combinations of energy sources that could form the proposed hybrid system were analyzed. The base-case was the fully dependent diesel powered network of 20.3 MW total installed capacity, 16.7 MW net available capacity and 13.4 MW peak demand in 2014. Others were diesel-PV and diesel-PV-Wind hybrids scenarios. Both PV and wind generators were modelled to 3 MW maximum capacity. Power systems simulation software, HOMER and DIgSILENT, were used to optimize the proposed hybrid system and integration to the existing network respectively.

The results indicated diesel-PV-Wind hybrid system as the most economically viable, having a reduced net present cost of 7 % in comparison with the diesel system and 5 % with the diesel-PV system. It also has the lowest cost of energy of 0.272 $/kWh. The result also indicated a significant impact of load distance on the voltage profile at the 11 kV and 33 kV feeders, in the absence of renewable sources. The farthest bus dropped below the nominal voltage by about 15 %, at 0.85p.u. However, with PV integrated at the farthest bus, the line load reduced and the system voltage improved but below the acceptable voltage limit of 0.92p.u. With the wind generator connected to the system, the

voltage improved further at the point of connection but remained constant around the weakest segments of the network. Finally, the PV was redesigned with voltage control to inject reactive power into the system. The result indicated an overall system voltage improvement that operated within acceptable designed limits. The weakest bus being 0.98p.u. The result of the assessment showed that renewables' integration is techno-economically beneficial to the existing power system network. However, grid integration of the renewable system was not considered. Thus, the effect of the system on the power losses, thermal and voltage profile of the distribution network was not carried out.

Dahiru *et al*. (2020), conducted a techno-economic analysis of a grid-connected nanogrid with PV, wind turbine, and battery storage systems for tropical climates of the Savannah. The system was designed for residential load of five households at Danladi Nasidi quarters, Kano, Nigeria. A 24 hours load demand of the households was obtained through survey and HOMER optimization software was used to conduct the analysis. The residential daily load demand of 355 kWh and 42 kW load profile in a 24 hour was obtained. The best optimal configuration obtained had 150 kW PV capacity, 4500 kW and 130 kW wind turbine and inverter components respectively. A comparative analysis of the techno-economic results obtained was achieved with the design carried out by(Dahiru and Tan, 2020) on standalone nano-grid system. A 98 % renewable fraction obtained was much higher by 28 % and the grid integration offers a solution to excess generation with potential for trade-offs. The result also showed lower greenhouse gas emission (GHG) of 2328 tons/year against 4000 tons/year. Economically, a much lower LCOE of -0.0110 $/kWh against 0.689 $/kWh and NPC of -$366,210 were obtained. Furthermore, the result is an indication of higher prospect for energy export to the existing

conventional grid network(Dahiru and Tan, 2020). However, the impact assessment on voltage profile, thermal loading and power losses were not conducted.

Olatomiwa *et al*. (2019) conducted a study that maximizes renewable penetration and minimizes cost of providing access to electricity for rural dwellers in achieving sustainable development goals (SDG). A rural healthcare centre was considered for the study and analysis was performed using HOMER software for techno-economic and environmental impact assessments. The demand side management (DSM) approach was also deployed to minimize the peak and average demand. For an average daily demand of 20.58 kWh, an optimum hybrid system configuration of PV/battery/Gen with 75 % reduction in CO_2 was obtained. The result also produced COE of 0.224 $/kWh, NPC of $61.917.6 with initial capital cost of $16,046.5. The optimal configuration obtained when the DSM was utilized produced lower values of COE, NPC and initial capital cost amounting to $0.166 /kWh, $18,614.7 and $10,070.8, respectively. Thus, substantial savings of 25.8 % and 70 % in COE and total NPC, respectively, were achieved for the health centre (Olatomiwa and Blanchard, 2019). However, the analysis lacked grid integration; thus, the impact assessment on voltage profile, thermal loading and power losses were not studied.

Bilal *et al.* (2016), examined the economics of wheeling energy from hybrid systems to Gadoon industrial load, Pehur, Pakistan using HOMER optimization software. Different hybrid scenarios including Grid-Hydro-PV-Wind, Grid-Hydro and Grid-based (non-renewable) systems were considered. The result obtained showed the Grid-Hydro-PV-Wind hybrid system as the most economical with 42.85 % and 33.98 % reduction in electricity tariff and grid energy consumption respectively. Due to the already installed

hydro component, the COE and grid purchase also reduced by 26.89 % and 63.32 % respectively. A high renewable fraction of 66 % was achieved from the system(Bilal *et al.*, 2016). However, the study was limited to industrial load and the impact of energy wheeling on voltage profile, power losses and thermal characteristics were not studied.

Ayadi *et al* (2018), carried out a techno-economic assessment of grid-connected PV system for the University Jordan. The Trnsys model simulation software was used to determine the final yield, conversion efficiency, simple payback period and internal rate of return (IRR) based on Build Operate and Transfer (BOT) and Engineering Procurement Construction (EPC) models. The results produced EPC as a better model with 3years payback period having 32 % IRR(Ayadi *et al.*, 2018). However, the impact of the system on voltage profile, losses and thermal loading were not studied.

Purohit *et al* (2018), performed a techno-economic assessment on 39 PV-grid projects in India, of capacities between 2 MW to 20 MW. PVsyst model was used to determine the energy yield and an average 20.33 % Capacity Utilization Factor (CUF) was obtained for all projects against the 19 % benchmark fixed by the country's central electricity regulatory commission. The data obtained from the project locations were also used to carry out technical simulation of static and dynamic solar irradiance. The dynamics showed a little lower capacity factor than the statics. The techno-economic result also showed mutual deviation ranging from -14 % to 27 % and -12 % to 31 %. The LCOE varied from INR 5.21 kWh to INR 5.88 kWh. The assessment showed a generally low performance of the PV projects(Purohit and Purohit, 2018). However, optimization of PV outputs was not studied and the impact on voltage and thermal loading was also not studied.

Azerefegn *et al*. (2020), carried out an analysis of grid-connected PV/Wind system to improve electricity supply reliability to Ethiopian industrial parks. Three industrial sites were considered to conduct the analysis using HOMER Pro software. Among the different scenarios analyzed, the grid/diesel/PV/wind/battery system was techno-economically viable for all the three locations. The cost of energy were 0.044, 0.049 and 0.048 $/kWh. CO_2 emission reduced by 45 %, 44 % and 42 %(Azerefegn *et al.*, 2020). However, the impact assessment on voltage profile, thermal loading and power losses were not studied.

Al Momani *et al* (2017), studied the impact of PV systems on voltage profile and power losses of 33 kV distribution networks in Al-Mafraq, Jordan. The PV total output of 10 MW integrated to the networks were analyzed using DigSILENT power factory. The analysis performed on the Salhyia 33 kV feeder of 7 MW before and after connection to PV output of 3 MW showed a decline in voltages with increased distance from the source. Highest value of 0.98p.u and least value of 0.94p.u were obtained when the PV component was not connected. The result indicated improvement in voltage profile when PV is connected with least value of 0.95p.u. Power losses significantly reduced from 7.01 % to 3.82 % before and after PV integration, respectively. Additional scenarios of PV output equal to and greater than load (by 50 %) were analyzed and the result displayed similar trend. The later, however produced higher losses (15.19 %) beyond the allowable limit of 11 % in distribution power system(Al Momani *et al.*, 2017) Similar studies conducted on the impact of high PV penetration on voltage profile and power losses produced similar results(Sultan *et al.*, 2019). However, the optimal PV output to be integrated was not ascertained as integration of existing capacities were analyzed and the system thermal effects were not studied.

The results of the above literatures reviewed consistently validate improvement in power system performance with integration of renewable DG. Grid-based integration with emphasis on system improvement and wheeling to industrial consumers have been implemented. However, wheeling to residential consumers leaves much to be desired. The impact of wheeling DG to a residential load of diverse and stochastic characteristics is yet to be comprehensively examined. Therefore, the aim of this research is to investigate the impact and viability of wheeling distributed generation of renewable resources from an IPP to residential loads, as an alternative approach to improved energy delivery using Gwarinpa Housing Estate, Abuja, as a case study. This will be carried out with the following objective in mind; To determine the optimum hybrid renewable energy potentials for DG that meet the case study residential loads, based on levelized cost of energy (LCOE) and net present cost (NPC) using HOMER., to determine the impact, and comparatively analyze the voltage profile, fault level, power losses and thermal loading of the case study distribution network with and without renewable DG integration using DIgSILENT and finally, determine the viability of energy wheeling to the residential load based on the outcome of these objectives.

CHAPTER 3

3.0 RESEARCH METHODOLOGY

This chapter presents the methodology adopted for the research study. The block diagram of the method adopted is shown in Figure 3.1. A detailed description of the components and the implementation flowchart is also presented. The solar and wind renewable energy assessment, load profile, and utility distribution network of the case study was obtained and presented.

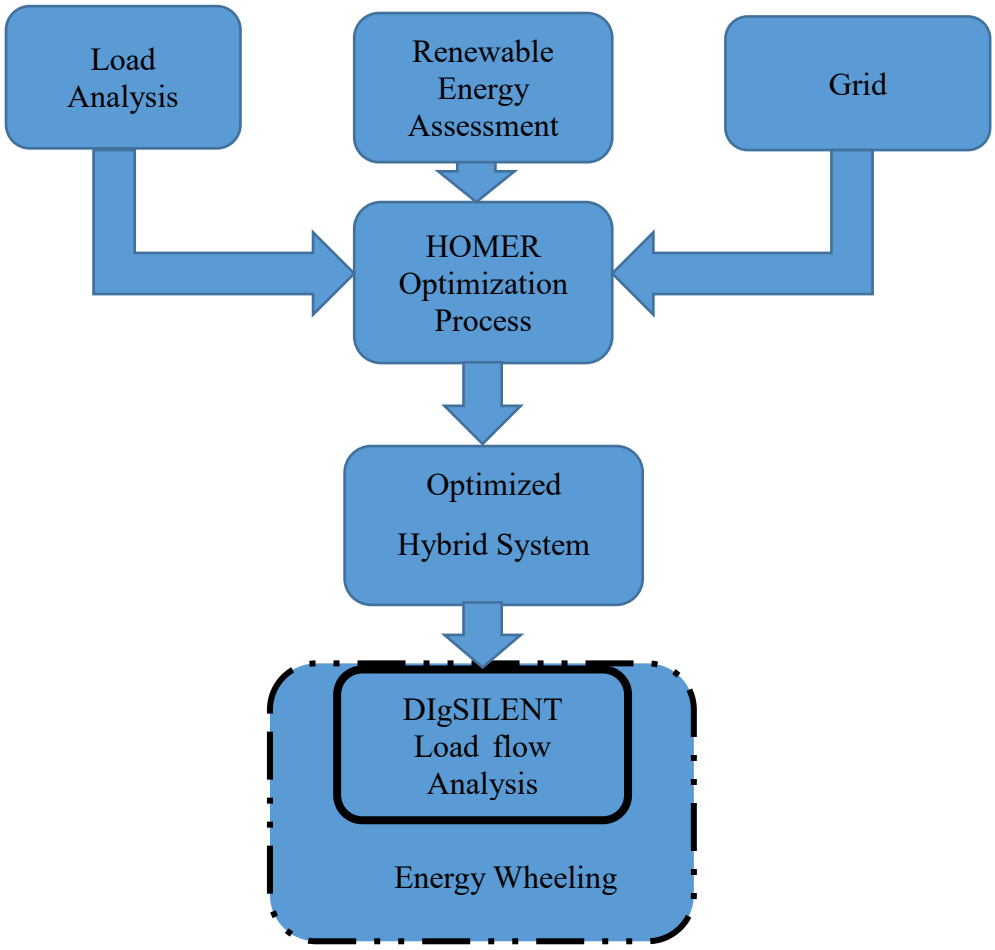

Figure 3.1: Block diagram of the method adopted

3.1 Methodology Framework

The methodology framework involves analysis of load consumption, assessment of renewable energy potential and the grid. These parameters formed the basis for the HOMER optimization process that produced the optimum hybrid system that meets the load demand of the estate. A load flow analysis was conducted to determine the impact of wheeling the renewable DG on the distribution network using DIgSILENT.

3.2 Load Pattern of Gwarinpa Housing Estate

The selected residential estate, Gwarinpa Housing Estate (GHE) Abuja, is mainly a residential area but consists of socio-economic businesses (Nnodu *et al.*, 2017). The load profile of the estate was obtained from the power supply utility companies viz the Transmission Company of Nigeria (TCN) and Abuja Electricity Distribution Company (AEDC). The hourly load consumption of the GHE for the year 2019/2020 was obtained, and average values for each hour for the month were computed as input for HOMER optimization. The average daily peak consumption of 13.997 MW was recorded at 1900 hours in June, and the average annual peak of 22.7 MW in the same month. The daily and monthly load profiles are shown in Figures 3.2 and 3.3, respectively.

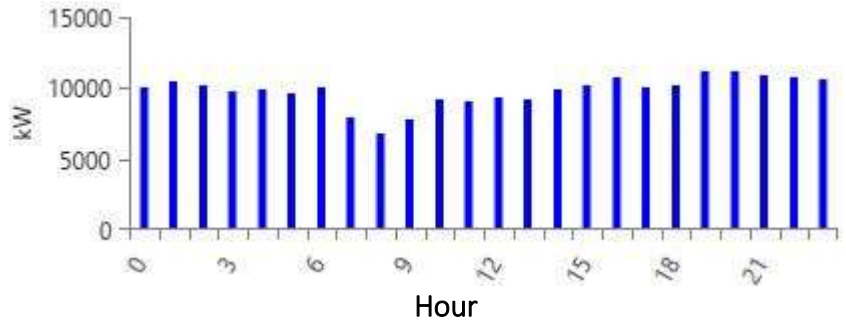

Figure 3.2: Daily load profile of GHE

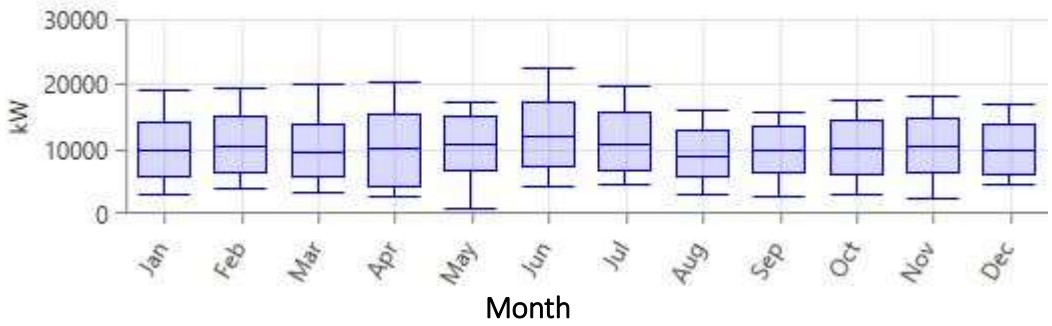

Figure 3.3: Monthly load profile of GHE

3.3 Models of Renewable Energy Resources

The renewable energy (RE) flow path is shown in Figure 3.4 (Infield and Freris, 2020). Some RE technology that may be available for the case study includes hydroelectric, photovoltaic (PV), wind, biofuels and so on. For this work, renewable energy resources of wind and solar PV were considered due to the comparative advantages of these sources to the research case study's geographical location, their abundance and ease of accessibility.

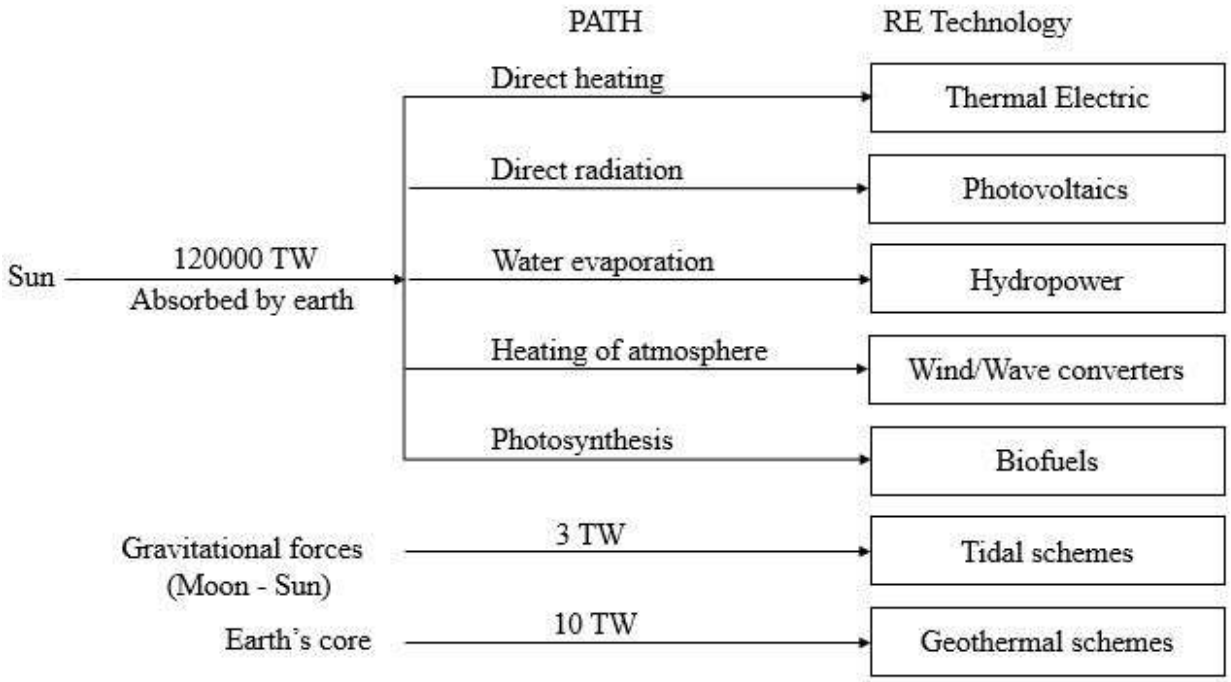

Figure 3.4: The renewable energy flow path (Infield and Freris, 2020).

3.3.1 Solar resources

Sun provides the major source of renewable energy that is easily harnessed. On average, solar radiation intercepted on the earth's surface amounts to about 8000 times the size of the global primary energy consumption rate of 500 EJ, equivalent to 1.4×10^{17} Wh (Infield and Freris, 2020). Nigeria, being a high solar insolation country has great potential for solar energy production. Abuja has an estimated monthly global solar radiation ranging between 129.9 kWh/m^2 to 194.4 kWh/m^2 and annual global solar radiation of 1988.8 kWh/m^2 (Agbetuyi *et al.*, 2018).

3.3.1.1 A*ssessment of the solar energy resources*

The potential for solar energy resources for the case study was determined using HOMER software. The monthly average solar global horizontal irradiance obtained from the National Solar Radiation Database, National Renewable Energy Laboratory (NREL) database is presented in Table 3.1. From the result, an annual average of 5.55 kWh/m^2/day was obtained.

Table 3.1: Solar energy resources for GHE

Month	Clearness Index	Daily Radiation (kWh/m^2/day)
January	0.630	5.673
February	0.585	5.641
March	0.605	6.209
April	0.582	6.114
May	0.553	5.727
June	0.512	5.219
July	0.455	4.654
August	0.455	4.722
September	0.501	5.159
October	0.599	5.865
November	0.653	5.949
December	0.643	5.628

3.3.1.2 M*athematical modeling of the photovoltaic system*

The equivalent circuit of the PV cell is shown in Figure 3.5

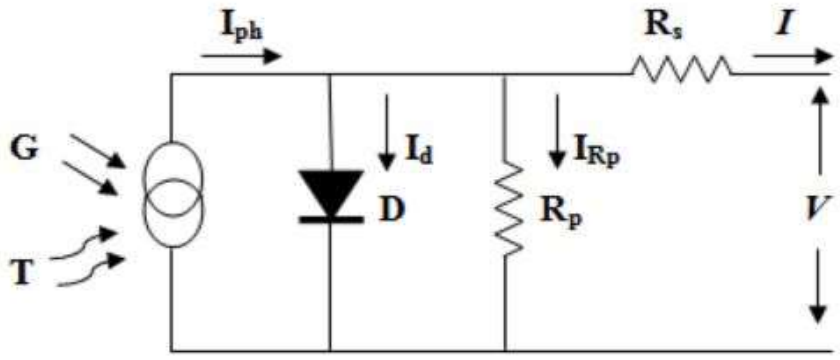

Figure 3.5: Single-diode equivalent circuit of a PV cell (Al Momani *et al.*, 2017).

Applying Kirchhoff's current law to the circuit of Figure 3.5, the output current of the PV module, I is given as (Al Momani *et al.*, 2017; Aoun and Bailek, 2019; Zaidi *et al.*, 2018).

$$I = I_{ph} - I_d - I_{R_p} \tag{3.1}$$

where I_{ph} is the photovoltaic (light-generated) module current, I_d is the current (voltage-dependent) lost due to recombination, and I_{R_P} is the current lost due to parallel or shunt resistance.

I_d modelled using Shockley Equation for an ideal diode, is given as;

$$I_d = I_o\left[\exp\left(\frac{V+IR_s}{nV_T}\right)-1\right] \tag{3.2}$$

where I_o is the reverse saturation current of the diode, V is the output voltage of the PV module, R_s is the series resistance, n is the ideality factor of the module which is a measure of deviation of the diode from the ideal factor Equation. V_T is the thermal voltage expressed as;

$$V_T = \frac{KT_O}{q} \tag{3.3}$$

where K is the Boltzmann's constant, T_o is the absolute temperature, and q is the electron charge.

The current lost due to parallel or shunt resistance, I_{R_P} is;

$$IR_P = \frac{V+IR_s}{R_P} \tag{3.4}$$

where R_P is the parallel or shunt resistance.

Thus, Equation (3.1) becomes;

$$I = I_{Ph} - I_o\left[\exp\left(\frac{V+IR_s}{nV_T}\right)-1\right]-\frac{V+IR_s}{R_P} \tag{3.5}$$

The power output of PV module is given as (Aoun and Bailek, 2019; Olatomiwa *et al.*, 2015)

$$P_o = P_r \times \left(\frac{G}{G_{ref}} \right) \times \left[1 + K_T \left(T_c - T_{ref} \right) \right] \tag{3.6}$$

where P_o is the PV cell power out, P_r is the PV cell rated power at reference condition, G is the solar radiation measured in W/m^2, G_{ref} is the solar radiation at standard temperature, given as; $G_{ref} = 1000W/m^2$. K_T is the temperature coefficient of the PV module, T_c is the PV cell temperature, expressed as; $T_c = T_{amb} + \left(0.0256 \times G \right)$, where T_{amb} is the ambient temperature. T_{ref} is the temperature of the cell at reference conditions, given as; $T_{ref} = 25^o C$.

3.3.2 Wind energy resources

Abuja has an annual mean wind speed of 3.244 m/s at hub height of 10 m (Owoeye *et al.*, 2017). However, the GHE site and meteorological data required for the simulation and optimization of PV/Wind hybrid energy generation system was imported from National Aeronautics and Space Administration (NASA) satellite measurement using HOMER optimization software.

3.3.2.1 *Assessment of the wind energy resources*

The National Aeronautic Space Agency (NASA) in HOMER software was deployed to generate the wind resources of GHE. An annual average wind speed of 3.01 m/s at anemometer height of 50 m was obtained. The detailed result is shown in Table 3.1

Table 3.2: Monthly average wind speed of GHE

Month	Average wind speed (m/s)
January	2.970
February	2.860
March	3.230
April	3.100
May	3.220
June	2.190
July	3.190
August	3.210
September	2.990
October	2.580
November	3.010
December	2.830

3.3.2.2 M*athematical modeling of the wind turbine*

The mean wind speed (MWS) is the commonly used parameter for determining wind energy potential. A wind speed of 3 m/s at 10m is viable for utility-scale wind farm. Mean wind speed is defined as (Owoeye *et al.*, 2017).

$$MWS = \frac{1}{n}\sum_{i=1}^{n} v_i \tag{3.7}$$

where n is the sample size and v_i is the speed of wind measured for the i^{th} time.

However, this wind power density is a better parameter for determining wind energy potential (Ahmed and Kunya, 2019). The mean wind power density P_w, is given as (Ahmed and Kunya, 2019; Olatomiwa *et al.*, 2015; Owoeye *et al.*, 2017).

$$P_w = \frac{1}{2}\rho v^3 \tag{3.8}$$

where ρ is the density of air $\left(1.225 kg/m^3\right)$, and v is the speed of the wind.

The mechanical power produced over an area from the conversion of wind energy by the wind turbine is expressed as;

$$P_m = \frac{1}{2}\rho A v^3 \tag{3.9}$$

where A = area.

The electrical power P_e obtained from the conversion is (Olatomiwa *et al.*, 2015).

$$P_e = \frac{1}{2} \times \rho \times P_{\max} \times A \times v^3 \times 10^{-3} \tag{3.10}$$

Where $P_{\max}$ is the maximum power extraction efficiency of the wind turbine system.

3.4 Hybrid System Modelling and Optimization

The HOMER Pro software was used to model and evaluate the optimal hybrid system based on the load consumption and meteorological data of GHE. HOMER software, has the capability to conduct simulation, optimization and sensitivity analysis of different scenarios to determine the optimal configuration for both off-grid and grid integrated systems and avail users the accessibility of techno-economic feasibility outcomes (Al Ghaithi *et al.*, 2017; Olatomiwa and Blanchard, 2019). The electric load was selected and the load profile of GHE was uploaded. Subsequently, the solar, wind and converter components were selected and their resources generated. The grid component was also selected and the techno-economic parameters including cost of electricity were uploaded. The simulation process is a performance modelling of hybrid configuration based on each

time step. The optimization process considers various scenarios in order to determine the configuration that fulfill system constraint at the minimum life-cycle cost (Magarappanavar and Koti, 2016). Sensitivity analysis involves performing different optimizations to determine the techno-economic impacts on the optimized system configurations. HOMER makes a comparative analysis of the energy generated by different configurations with the load profile, every hour for the year. The NPC, operating cost and the LCOE optimal configuration that meets the load demand is then computed (Al Ghaithi *et al.*, 2017; Kumar and Deokar, 2018; Lipu *et al.*, 2017; Radzi *et al.*, 2019).

3.5 The Gwarinpa Housing Estate Distribution Network

Gwarinpa Housing Estate (GHE) is powered from the national grid via a 9-bus distribution network comprising of two transmission and three distribution substations as shown in Figure 3.6. From the source, Katampe 132/33 kV transmission substation, a 60 MVA transformer supplies electricity to GHE via a 15 km, 33 kV Gwarinpa feeder. Similarly, the 132/33 kV Kubwa substation, located at Dutse area of Abuja, is about 11.4 km transmission line, away from the source 132 kV bus at Katampe. Electricity flows from the substation's 60 MVA transformer to GHE via an 8 km, 33 kV Dawaki feeder. Furthermore, Gwarinpa feeder connects two 33/11 kV distribution substations, 2 x 15 MVA and 1 x 15 MVA capacities. While Dawaki feeder connects 1 x 15 MVA, 33/11 kV substation, all located within the estate. A total number of 8 x 11 kV load feeders distributes electricity in the estate as shown in Table 3.2. The 33 kV and 11 kV voltage level of the utility distribution network served as the base network for this research. The integration of the renewable DG system was implemented at this level. The network operates at a national frequency of 50 Hz ±0.5 % under normal condition, and ±2.5 % under system stress. The distribution voltage limit of 0.95p.u to 1.05p.u and maximum

allowable thermal loading of 80 % (NERC, 2018). For energy wheeling to be viable, the distribution network parameters are expected to maintain operational limits.

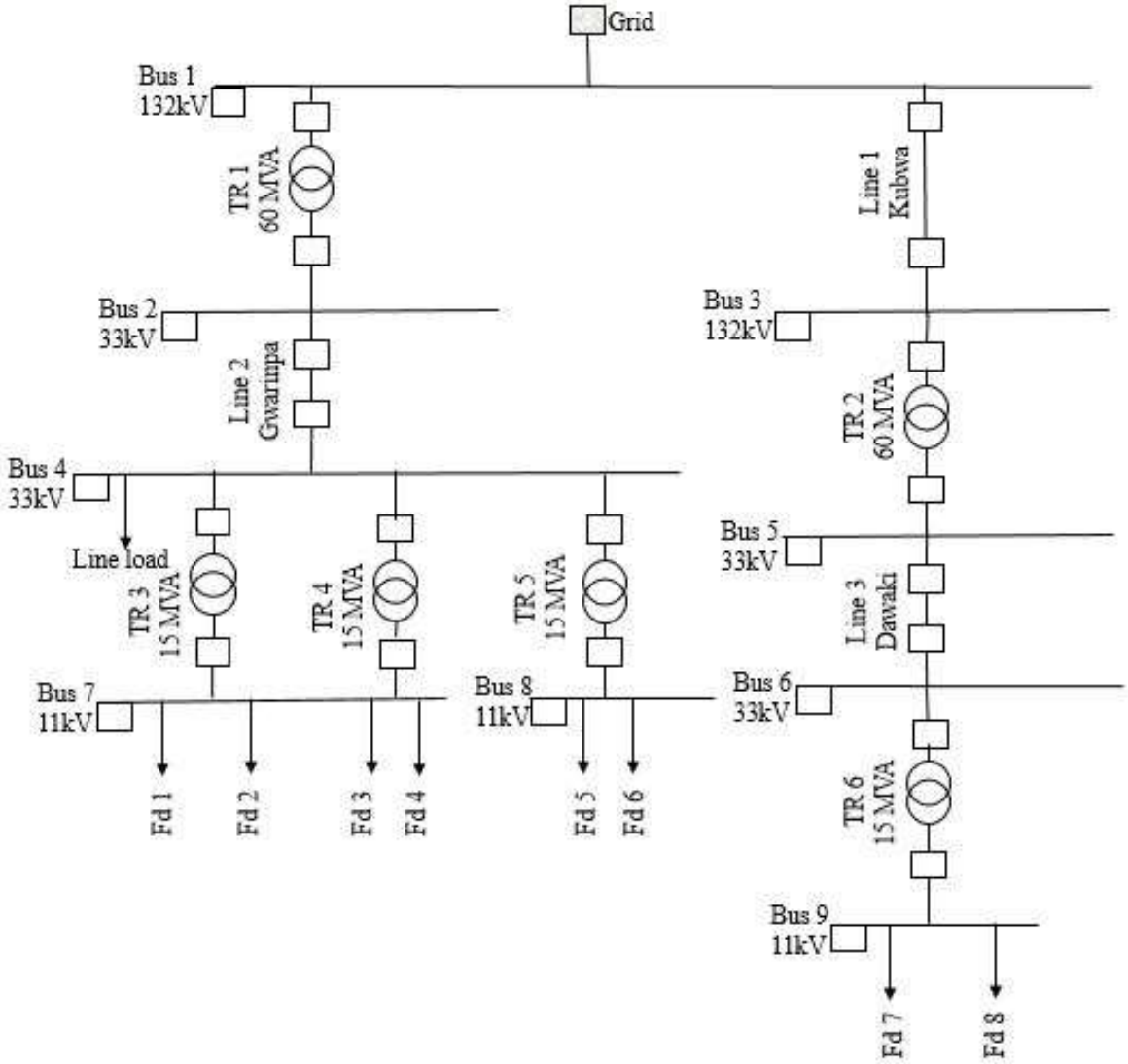

Figure 3.6: The 9-bus distribution network of GHE.

Table 3.3: Specifications of the distribution network for GHE.

Component	**Name**	**Specification**
Transmission Line	Line 1 (Kubwa)	Line length = 11.4 KM, I_r = 1200 A, r = 0.176 Ω/km, x = 0.392Ω/km, V_r = 132kV,
Transmission Substations	Katampe	Txf_1 = 60 MVA, 132/33kV, Vector group = Dyn11
	Kubwa	Txf_2 = 60 MVA, 132/33kV, Vector group = Dyn11
Feeders	Gwarinpa (Line 2)	Line length = 15 km, V_r = 33kV, I_r = 600 A, r = 0.015 Ω/km, x = 0.3 Ω/km
	Dawaki (Line 3)	Line length = 8 km, V_r = 33kV, I_r = 600 A, r = 0.015 Ω/km, x = 0.3 Ω/km
Distribution Substations	M42	Txf_3 = 15 MVA, 33/11 kV, Vector group = Dyn11, Txf_4 = 15 MVA, 33/11 kV, Vector group = Dyn11,
	M43	Txf_5 = 15 MVA, 33/11 kV, Vector group = Dyn11,
	M44	Txf_6 = 15 MVA, 33/11 kV, Vector group = Dyn11,
Loads	K5 (Fdr 1)	L = 5.17 MW, pf = 0.80, V(p.u) = 1
	K6 (Fdr 2)	L = 3.65 MW, pf = 0.80, V(p.u) = 1
	K12 (Fdr 3)	L = 3.28 MW, pf = 0.80, V(p.u) = 1
	K14 (Fdr 4)	L = 4.05 MW, pf = 0.80, V(p.u) = 1
	Adkan (Fdr 5)	L = 3.28 MW, pf = 0.80, V(p.u) = 1
	Setraco (Fdr 6)	L = 2.5 MW, pf = 0.80, V(p.u) = 1
	Fdr 1 (Fdr 7)	L = 4.32 MW, pf = 0.80, V(p.u) = 1
	Fdr 2 (Fdr 8)	L = 1.10 MW, pf = 0.80, V(p.u) = 1

3.6 Simulation and Load Flow Analysis

DIgSILENT software was used to carry out assessment of the impacts that could be created as a result of integration of the DG system. The software uses Newton-Raphson algorithm and convergence was obtained after three iterations. The software efficiently combines both classical power system analysis with modern power system tools. The loads were modelled as general loads, that is, all non-motor loads, as provided by the software. Impact analysis focused on the test distribution network's voltage profile, fault level, power losses and thermal loading.

Subsequently, three different DG connection scenarios were considered for the study based on the test case load flow outcome. The buses with the lowest magnitudes of voltage were identified and formed the connection scenarios. Scenario 1 consists of buses 7 and 8, scenario 2 has buses 7, 8 and 9, while scenario 3 has only bus 4. The nominal system parameters are 50 Hz ±0.5 %, voltage from 0.95p.u to 1.05p.u and maximum loading of 80 %. The DG was modelled to meet the load requirement of the busbars. The DGs, denoted as PV, PV(1), PV(2) and PV(3) systems, with multiple paralleled inverters, were connected to buses 7,8,9 and 4, respectively.

An inverter of 2500 kVA with a power factor of 0.75 was chosen to model the single PV system that produced an approximate output of 1875 kW at 77 % loading. All the PV systems listed are of equal size, but the output connected to the buses differ due to variation in the number of paralleled inverters that meets the buses load requirement, as shown in Table 3.4. For each scenario, comparison with the existing utility network was made to determine the impact on voltage profile, line losses, fault contribution and

thermal loading. The three scenarios were independently investigated. That is, when the first scenario was active, the PV systems of the second and third scenarios were shutdown.

Table 3.4: Specifications of the PV Systems

PV System	Active Power (kW)	No. of parallel inverters	Local Controller	Output Power (kW)
PV	1875	10	Voltage	18750
PV(1)	1875	5	Voltage	9375
PV(2)	1875	5	Voltage	9375
PV(3)	1875	15	Voltage	28125

Finally, distances in form of overhead lines were introduced between the load buses and the PV systems based on the location of the industrial sites around GHE. Idu phases 1 and 2 which are between 5 and 7 km, and Idu phases 3 and 4, between 7 and 10 km. For this study, 5 and 10 km were considered as the possible location for DG sites by the IPPs.

PV, PV(1) and PV(2) were connected to the grid distribution substation bus 7, 8 and 9 via overhead lines 5 km long. The PV, PV(1) and PV(2) and PV(3) systems were connected to DG buses denoted as PB1, PB2, PB3 and PB4 at the site, from where the overhead lines denoted as PV line, PV line1, PV line2 and PV line3 respectively, takes supply. Load flow were conducted at 5 km based on the three scenario connections and results obtained. The same procedure was repeated with overhead lines 10 km long, and all results obtained were compared with the distribution network without PV connection. Thus, the impact of the distance between the DG (PV) site and the load on the voltage profile, thermal loading, fault level and line losses of the GHE distribution network were ascertained.

3.7 Implementation of the Methodology

A flowchart of the implementation process shown in Figure 3.7 was executed to obtain the desired result.

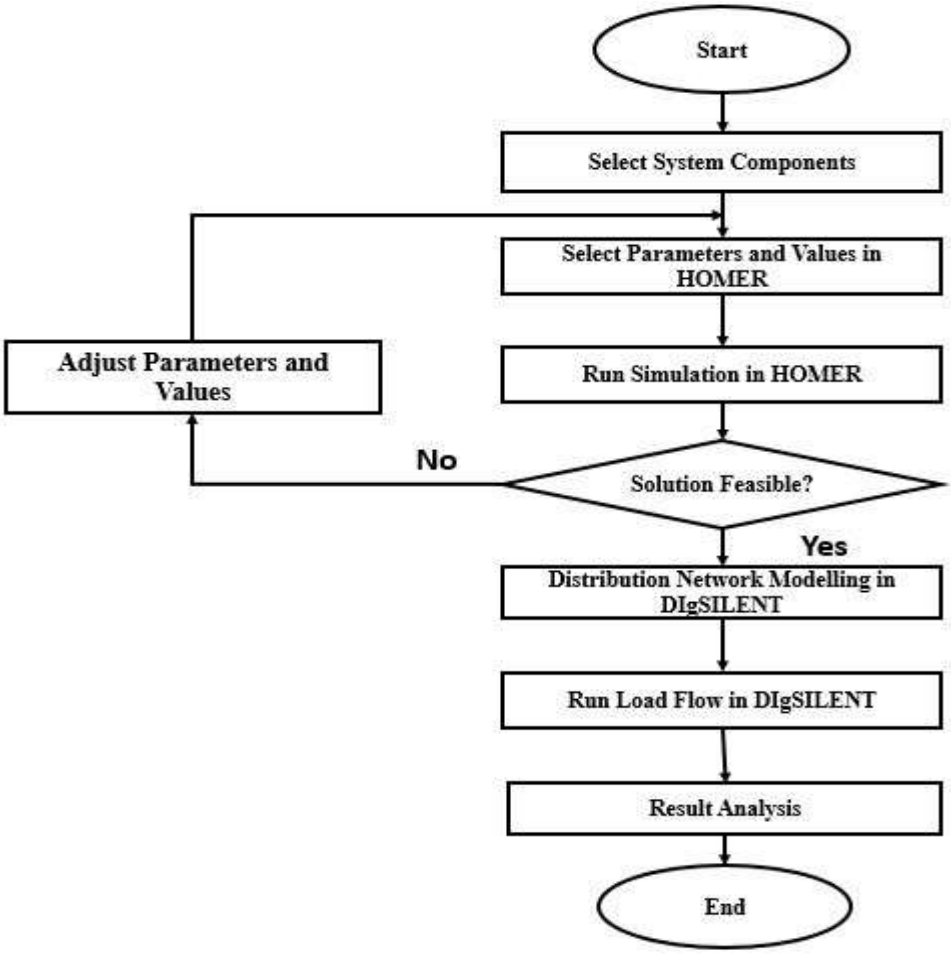

Figure. 3.7: Flowchart of the implementation process.

CHAPTER FOUR

4.0 RESULTS AND DISCUSSION

This chapter presents the result of the research study based on the methodology highlighted in chapter three. The system architecture of the optimal configuration obtained from HOMER optimization is presented. The load flow result of the utility distribution network of the case study, with and without DG is also shown and discussed. The results of the various DG connection scenarios corresponding to the utility voltage profile, thermal loading, line losses and fault levels are also presented and analyzed. Finally, the results are compared and the viability of connecting DG to the utility network for energy wheeling to GHE is determined.

4.1 The Optimal System Configuration

The resultant optimal system architecture obtained from HOMER, is shown in Figure 4.1. The optimal configuration is made of grid/PV/converter, with Net Present Cost (NPC) and Levelized Cost of Energy (LCOE) of $72.4 million and $0.0188 respectively.

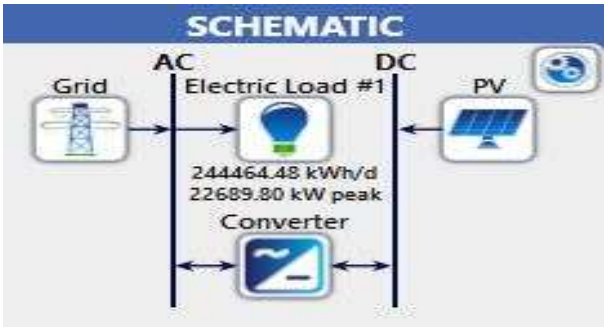

Figure 4.1: Optimal System architecture

The optimum system excludes wind due to the low potential for energy generation around the case study. An average wind speed of 3.01 m/s obtained is not sufficient for viable

output that requires a minimum average of 3.4 m/s. Thus, further study on the impact analysis was based on the optimal system configuration of Figure 4.1

4.2 Load Flow of the GHE Distribution Network

The load flow was successfully executed on the one-line diagram of the GHE distribution network of Figure 3.6. The resultant distribution network is shown in Figure 4.2. The result shows that bus 4 is on lower voltage limit of 0.95p.u while buses 7 and 8 were 0.94, below the lower limit. The result also shows 81.2 % loading of 33 kV Gwarinpa line, against the maximum of 80 %. The orange colour shows the overloaded line while the blue colour shows parts of the network with low voltage.

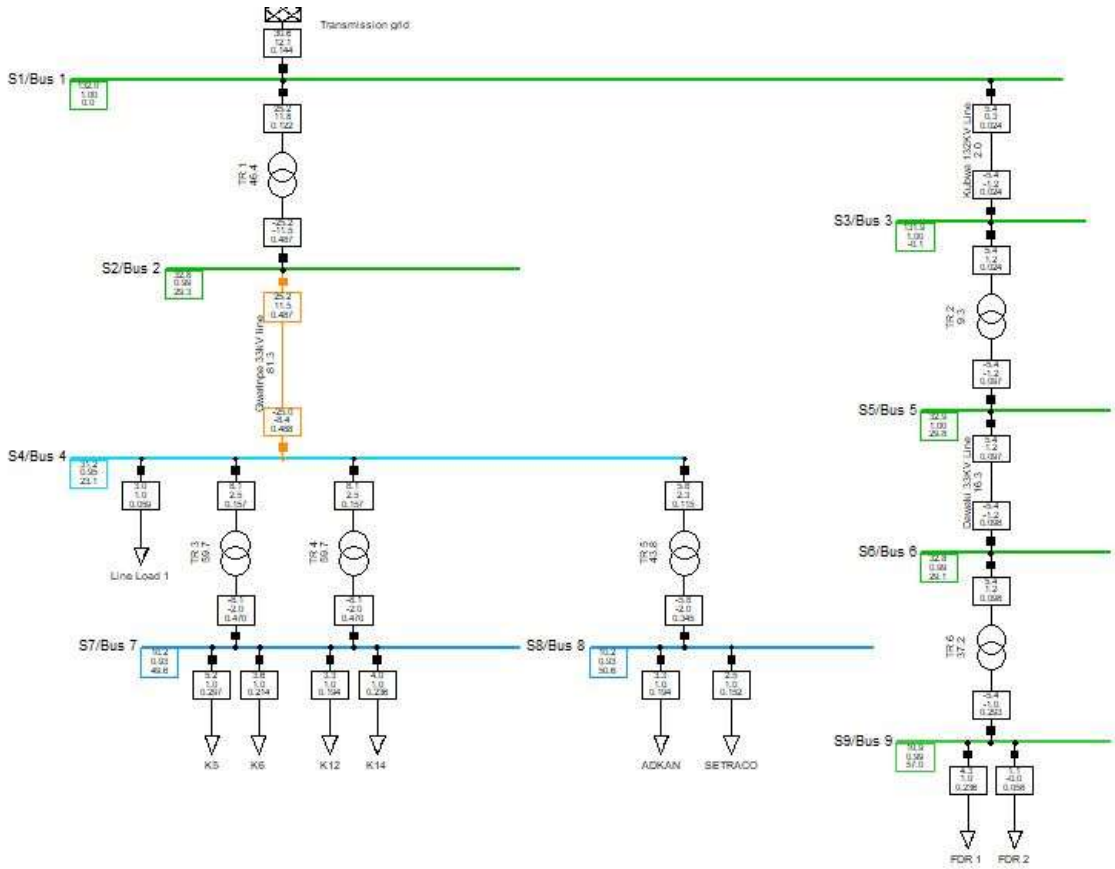

Figure 4.2: The load flow graphic of GHE distribution network.

4.2.1 Voltage profile of the GHE distribution network

The result of the voltage profile obtained from the load flow analysis of the GHE distribution network without PV connection is shown in Figure 4.3.

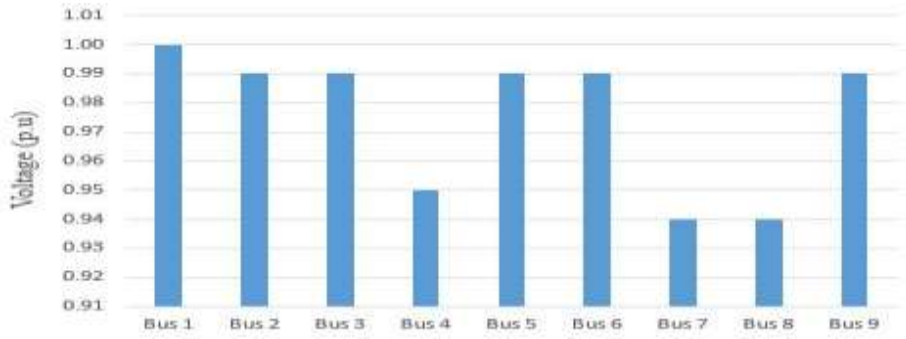

Figure 4.3: Voltage profile of the 9-bus GHE distribution network

From the voltage profile, the lowest voltage of 0.94p.u and highest value of 1.00p.u was obtained. While most buses had voltages within the allowable specification, buses 7 and 8 recorded the lowest voltage of 0.94p.u, in violation of the lower limit. Conventionally, the network voltage decreases with an increased distance from the source substation.

4.2.2 Fault level of the GHE distribution network

The short circuit current of the conventional network is calculated as a vital component for determining the network's current carrying and thermal capability. Figure 4.4 shows the initial short circuit current of the GHE distribution network.

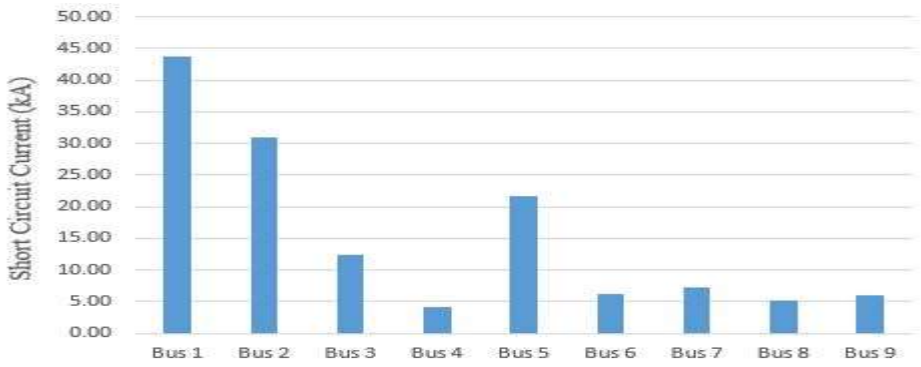

Figure 4.4: The initial short circuit current of the 9-bus GHE distribution network

Bus 1, 132 kV, recorded 43.74 kA, while the lowest fault occurred on bus 4, with a value of 4.04 kA. Generally, the magnitude of the low-voltage bus bars were minimal.

4.2.3 Thermal loading of the GHE distribution network

Figure 4.5, shows the thermal loading of the lines and transformers obtained from the load flow simulation of the GHE distribution network.

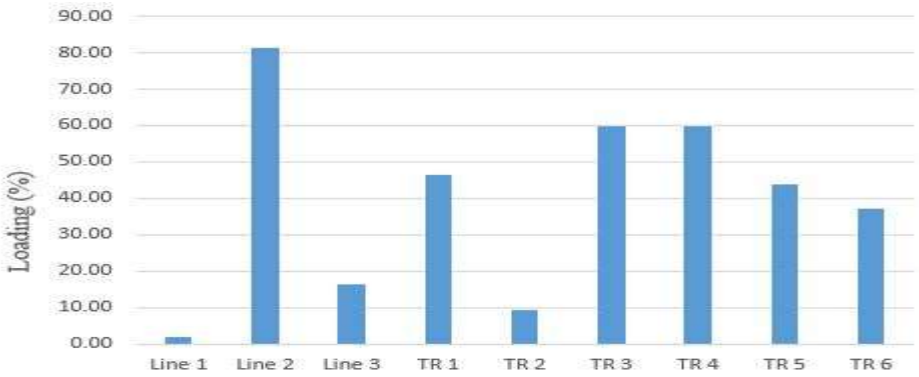

Figure 4.5: Thermal loading of the 9-bus GHE distribution network equipment.

Line 2 connecting buses 2 and 4 recorded 81.26 % loading, contrary to maximum limit of 80 %. This is expected as the line provides bulk of power supply to the estate being understudy. This overload could adversely contribute to the line losses, temperature and stress on insulation.

4.2.4 Line losses of the GHE distribution network

The active and reactive power losses of the GHE distribution network lines obtained from the load flow simulation result is shown in Figure 4.6. Lines 1, 2 and 3 denotes 132kV Kubwa, 33kV Gwarinpa and 33 kV Dawaki respectively. Line 2 had the highest active and reactive power losses among the three lines, with an approximate value of 0.199 MW and 3.11 MVAR respectively.

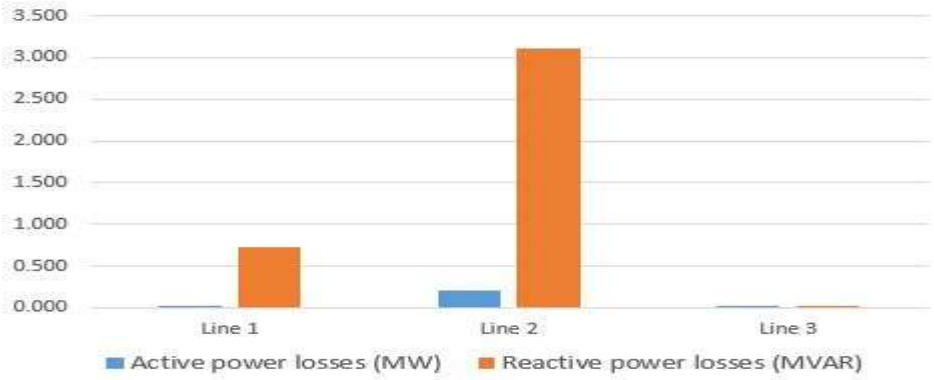

Figure 4.6: Line losses of the 9-bus GHE distribution network

The overloaded state of line 2, seen from the load flow result, explains why losses were much. However, active power loss was minimal on the three lines as seen from the graph.

4.3 Load Flow of the DG-Connected GHE Distribution Network

The load flow of the DG-connected GHE distribution network was carried out with DIgSILENT software, as shown in Figure 4.7. The solar PV simulated to meet the load requirement of the buses, as contained in chapter three was implemented, and the following results were obtained.

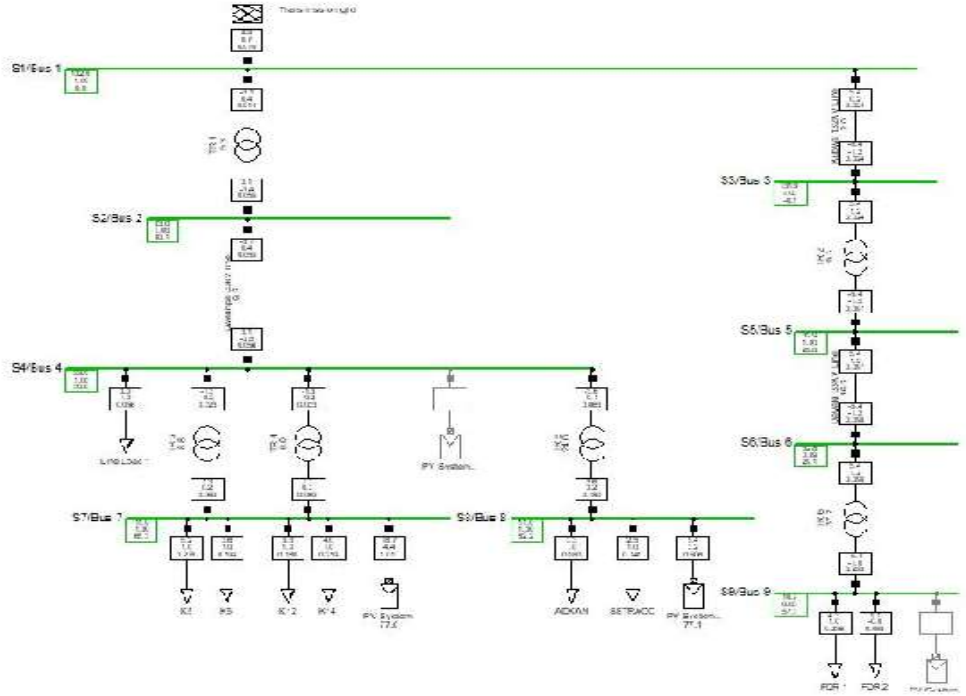

Figure 4.7: The load flow graphic of the PV-connected GHE distribution network.

4.3.1 Impact of PV system on voltage profile of the GHE distribution network

i. First scenario: PV system connected to bus 7 and 8

PV and PV(1) were connected to buses 7 and 8, respectively, and the load flow result shows improvement in bus voltages. The voltage profile obtained was compared with the voltage profile of the network before DG connection (Figure 4.3), as shown in Figure 4.8

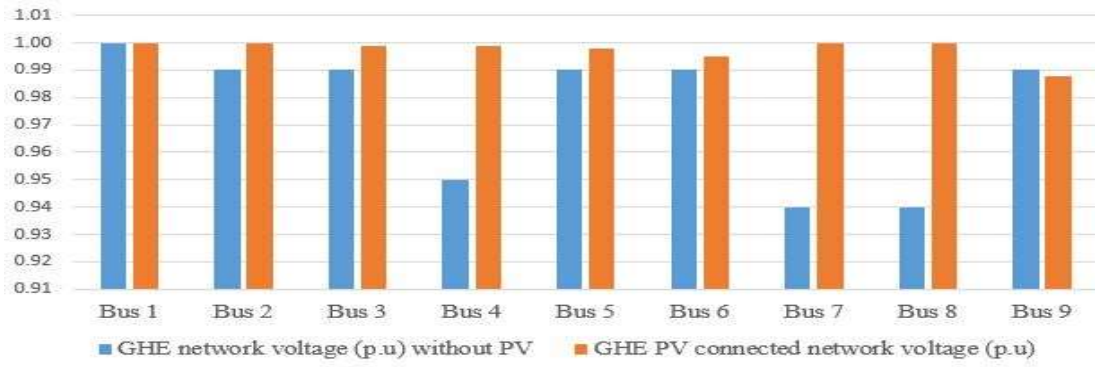

Figure 4.8: Voltage profile of GHE distribution network with and without DG connection (PV system connected to bus 7 and 8)

Obviously, PV integration brought about significant voltage improvement, with all the busbars operating within the allowable limits. Bus 7 and 8 that erstwhile had 0.94p.u, improved to approximately 1.0p.u. Supply voltage at rated values or within allowable limits is the desire of electricity consumers.

ii. Second scenario: PV system connected to bus 7, 8 and 9

For the second PV connection scenario, buses 7, 8 and 9 were connected with PV systems. PV(2) denotes the PV system connected to bus 9. The result obtained and the comparison with distribution network without PV, is shown in Figure 4.9

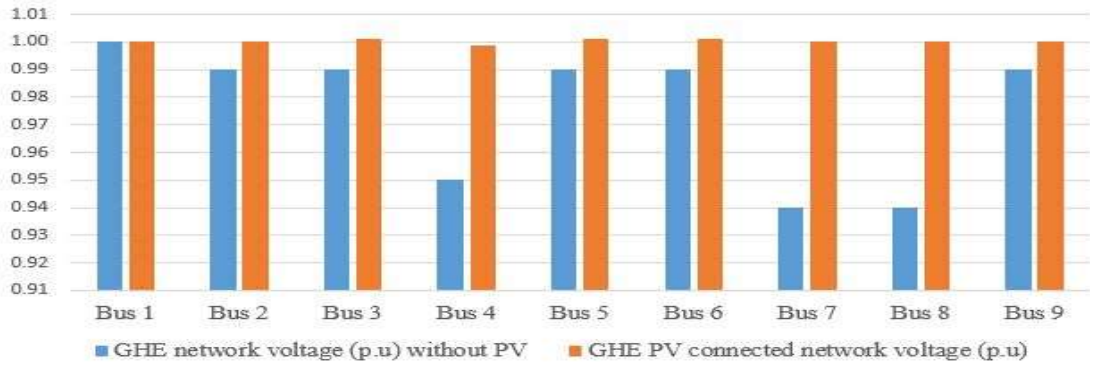

Figure 4.9: Voltage profile of GHE distribution network with and without DG connection (PV system connected to bus 7, 8 and 9)

The result obtained showed significant improvement of voltage on the busbars. The magnitude of the voltages increased to 1.00p.u approximately.

iii. Third scenario: PV system connected to bus 4

Only bus 4 was connected with PV system denoted as PV(3). The bus had a lower limit voltage of 0.95p.u for the test distribution network. The result obtained, and comparison with the GHE distribution network without PV, is shown in Figure 4.10

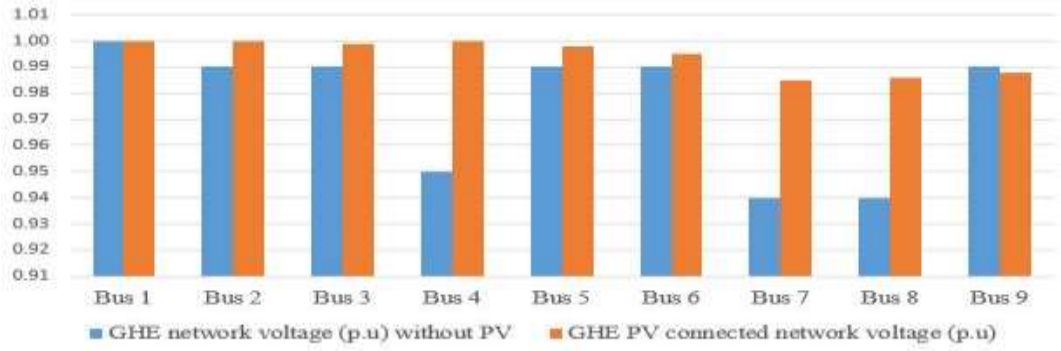

Figure 4.10: Voltage profile of GHE distribution network with and without DG connection (PV system connected to bus 4)

Significant improvement were observed on the busbars, with magnitudes approximately 1.00p.u. None of the buses dropped below the allowable limit of 0.95p.u.

4.3.2 Impact of PV system on fault level of the GHE distribution network

i. First scenario: PV system connected to bus 7 and 8

The PV systems denoted as PV and PV(1) were connected to buses 7 and 8 respectively. The result obtained and the comparison with the distribution network without PV, is shown below, Figure 4.11

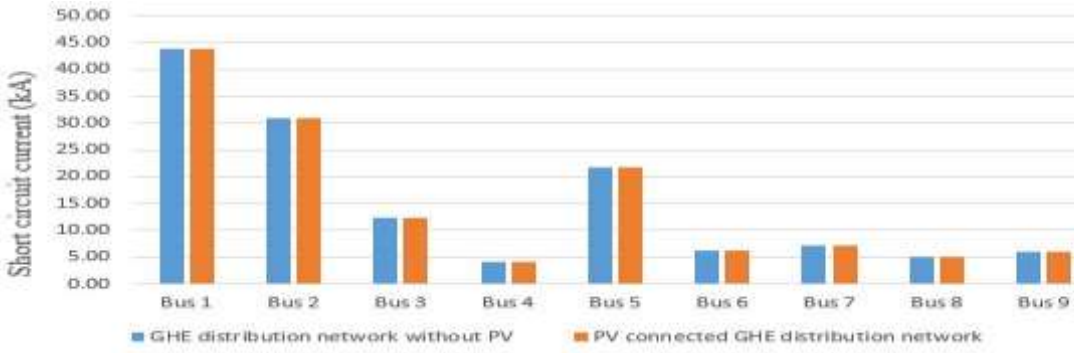

Figure 4.11: Fault level of GHE distribution network with and without DG connection (PV system connected to bus 7 and 8)

The result from the comparison showed no visible difference in fault level of the network. Inverter-based DG have minimal fault effect on the network, unlike the synchronous-based DG (Murray, 2018).

ii. Second scenario: PV system connected to bus 7, 8 and 9

For the second PV connection scenario, buses 7, 8 and 9 were connected with PV systems. PV(2) denotes the PV system connected to bus 9. The result obtained, compared with the distribution network without PV, is shown in Figure 4.12

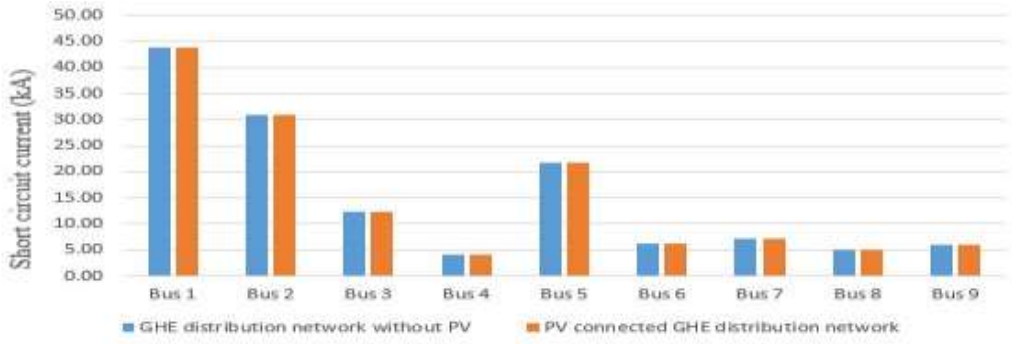

Figure 4.12: Fault level of GHE distribution network with and without DG connection (PV system connected to bus 7, 8 and 9)

A result similar to the first scenario was obtained. No visible fault contribution was observed.

iii. Third scenario: PV system connected to bus 4

Only bus 4 was connected with PV system denoted as PV(3). The bus had a lower limit voltage of 0.95p.u for the test distribution network. The result obtained and comparison with the test distribution network without PV, is shown in Figure 4.13

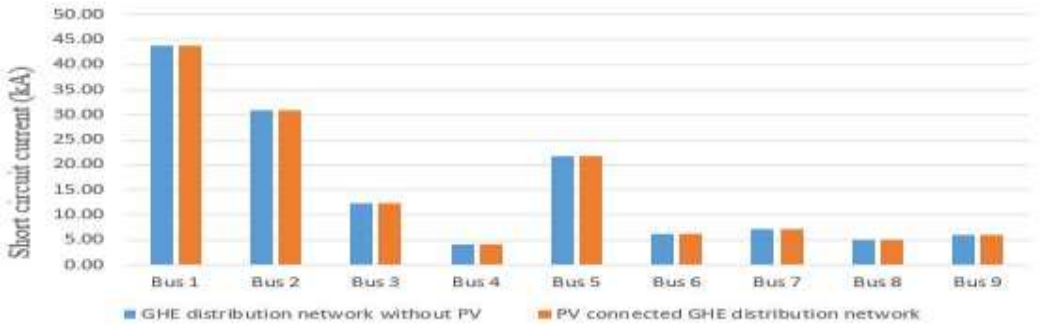

Figure 4.13: Fault level of GHE distribution network with and without DG connection (PV system connected to bus 4)

The result of this scenario exhibits the same trend as the first and second. No visible difference between the fault levels of the two networks.

4.3.3 Impact of PV system on thermal loading of the GHE distribution network

i. First scenario: PV system connected to bus 7 and 8

PV systems denoted as PV and PV(1) were connected to buses 7 and 8 respectively. The result obtained and the comparison with the distribution network without PV, is shown below, Figure 4.14

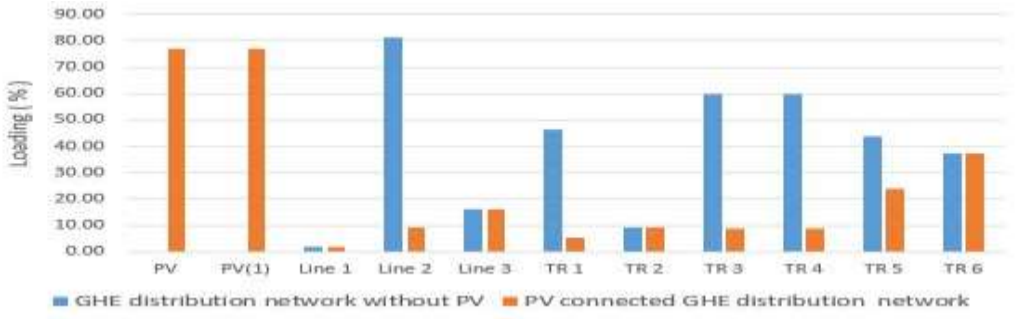

Figure 4.14: Thermal loading of GHE distribution network with and without DG connection (PV system connected to bus 7 and 8).

The result showed significant relief for the overloaded line 2. The line dropped from 81.26 % to 9.29 %. The reason is that PV systems provided additional power to the load that erstwhile depended solely on line 2. Thus, the impact of additional capacity created by the PV system was validated. The loading of other equipment was also reduced except for lines 3, TR2 and TR6, where no impact occurred.

ii. Second scenario: PV system connected to bus 7, 8 and 9

For the second PV connection scenario, bus 7, 8 and 9 were connected with PV systems. PV(2) denotes the PV system connected to bus 9. The result obtained and the comparison with the distribution network without PV, is shown in Figure 4.15

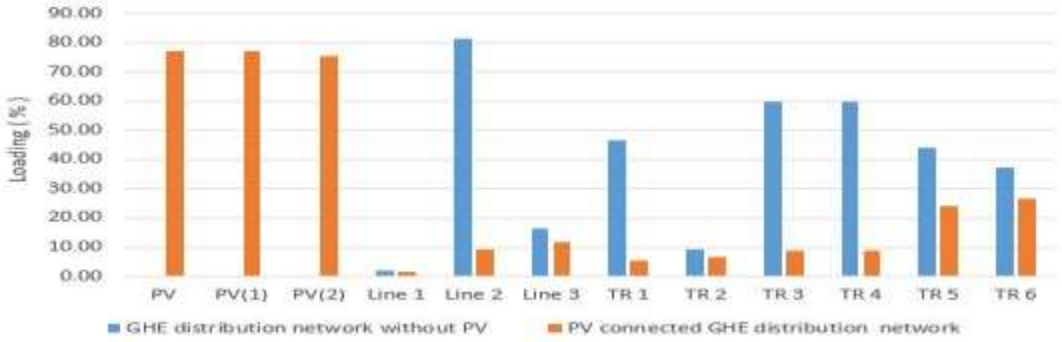

Figure 4.15: Thermal loading of GHE distribution network with and without DG connection (PV system connected to bus 7, 8 and 9).

The result showed similar trend with the first scenario. However, impact was observed on line 3, TR2 and TR6 unlike in the first scenario. Line 3 dropped from 16.27 % to 11.53 %, while TR2 and TR6 reduced from 9.28 % to 6.59 % and 37.21 % to 26.37 % respectively. No part of the network suffers from overload and therefore free from its adverse effects.

iii. Third scenario: PV system connected to bus 4

Only bus 4 was connected with PV system denoted as PV(3). The bus had a lower limit voltage of 0.95p.u for the test distribution network. The result obtained, and a comparison with the distribution network without PV, is shown in Figure 4.16

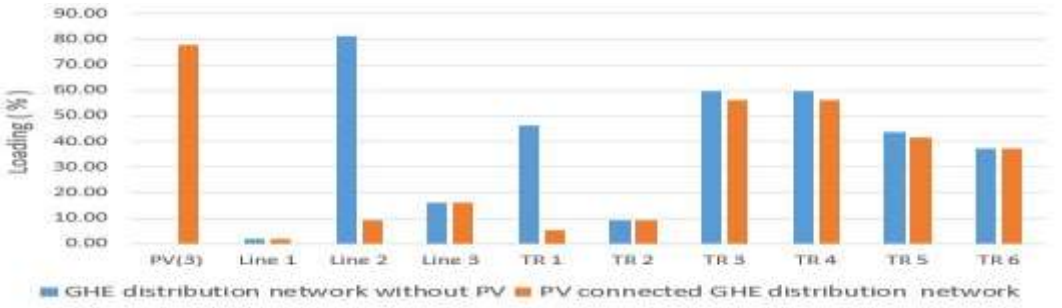

Figure 4.16: Thermal loading of GHE distribution network with and without DG connection (PV system connected to bus 4).

The result of this scenario is in line with the two previous scenarios where loading of the network was minimized with the integration of PV systems for energy wheeling. Line 2, TR1, TR3, TR4, and TR5, reduced from 81.26 %, 46.38 %, 59.69 %, 59.69 %, 43.84 %

to 9.19 %, 5.24 %, 56.31 %, 56.31 % and 41.37 % respectively. No visible change was observed on the others.

4.3.4 Impact of PV system on the GHE distribution network line losses

i. First scenario: PV system connected to bus 7 and 8

PV systems denoted as PV and PV(1) were connected to bus 7 and 8 respectively. The result obtained and the comparison with the distribution network without PV integration, is shown in Figure 4.17

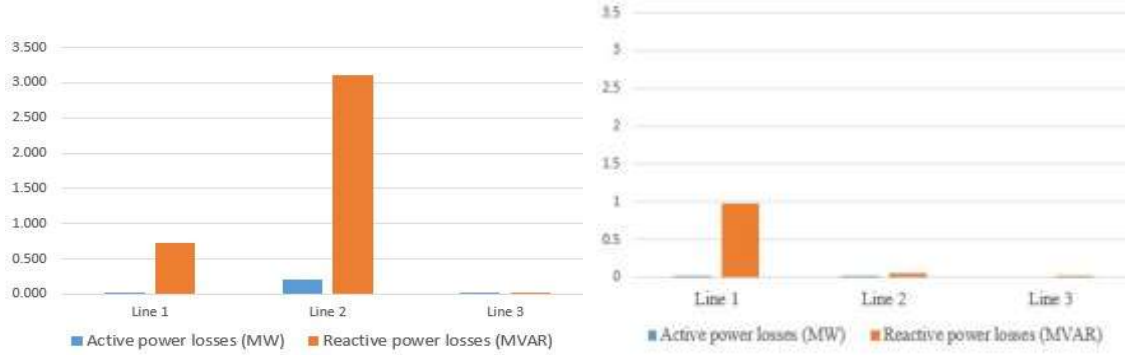

(a) (b)

Figure 4.17: Line losses of the GHE distribution network (a) without PV connection (b) PV system connected to bus 7 and 8

A significant impact was observed here due the additional DG capacity. On Line 2, active power loss dropped from 0.199 MW to 0.01 MW, while reactive power loss dropped from 3.11 MVAR to 0.06 MVAR. The additional capacity brought about by the integration of PV systems, relieved the erstwhile overloaded line 2 and thus, the reduction in losses. However, reactive power loss increased on line 1, from 0.73 MVAR to 0.98 MVAR.

ii. Second scenario: PV system connected to bus 7, 8 and 9

For the second PV connection scenario, bus 7, 8 and 9 were connected with PV systems. PV(2) denotes the PV system connected to bus 9. The result obtained and the comparison with the distribution network without PV, is shown in Figure 4.18

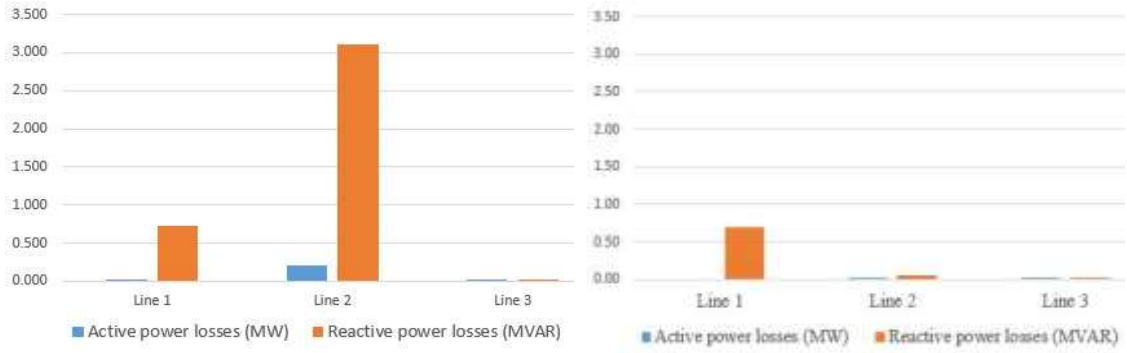

(a) (b)

Figure 4.18: Line losses of the GHE distribution network (a) without PV connection (b) PV system connected to bus 7, 8 and 9

The results were observed to show similar trend as the first scenario. On line 2, reduction in reactive power loss from 3.11 MVAR to 0.06 MVAR, while active power loss dropped from 0.199 MW to 0.01 MW. However, reactive power loss also decreased from 0.73 MVAR to 0.69 MVAR on line 1.

iii. Third scenario: PV system connected to bus 4

Only bus 4 was connected with PV system denoted as PV(3). The bus had a lower limit voltage of 0.95p.u for the test distribution network. The result obtained, and a comparison with the distribution network without PV, is shown in Figure 4.19

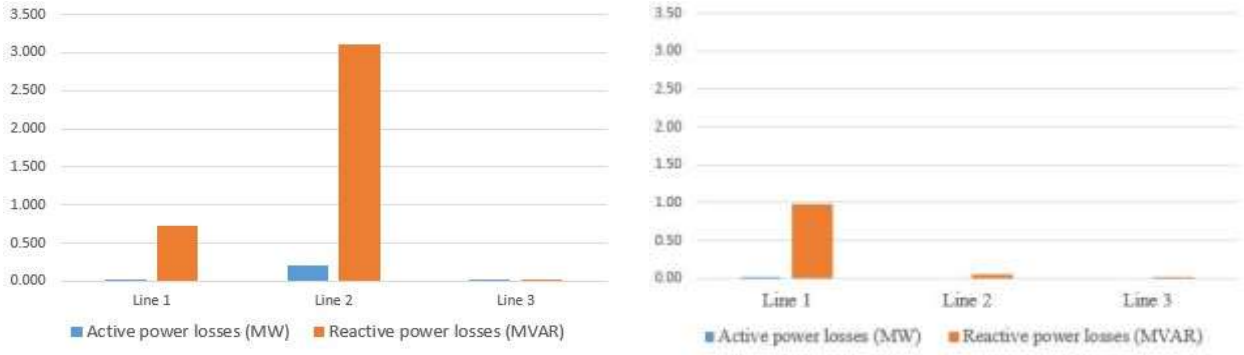

(a) (b)

Figure 4.19 Line losses of the GHE distribution network (a) without PV connection (b) PV system connected to bus 4

The result showed increase in reactive power from 0.73 MVAR to 0.99 MVAR on line 1. However, reactive power reduced on lines 2 and 3 from 3.11 MVAR and 0.012 MVAR to 0.06 MVAR and 0.01 MVAR respectively.

4.4 Impact of Distance between DG (PV) Site and the Load on the GHE Distribution Network

The result of the load flow of the PV-connected GHE distribution network under variant distances between the PV site and the load, conducted to investigate the impact on the performance indices, is presented as follows.

4.4.1 Impact of distance between DG (PV) site and the load on voltage profile of the GHE distribution network

i. First scenario: PV systems connected to bus 7 and 8

The comparison of the results obtained is shown in Figure 4.20.

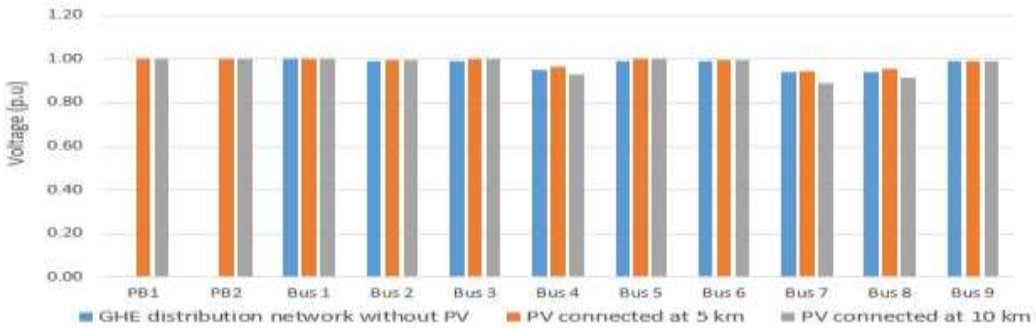

Figure 4.20: The impact of distance on voltage profile of PV connected GHE distribution network (PV connected to bus 7 and 8)

From the result, distance negatively impacted voltage profile and was even more at 10 km. Bus 7 that earlier improved to 1.00p.u before the distance was considered, dropped to 0.94p.u and 0.89p.u at 5 km and 10 km respectively. Both values violated the lower limit of 0.95p.u, but more severe at 10 km.

ii. Second scenario: PV systems connected to buses 7, 8 and 9

The result obtained is shown in Figure 4.21. This scenario produced a similar result to the first, bus 7 was still critically low at 10 km. The voltage on bus 8 dropped to 0.96p.u at 5 km, slightly above the lower limit and dropped deeper to 0.91p.u. Similarly, the voltage on bus 4, 0.93p.u dropped below the lower limit.

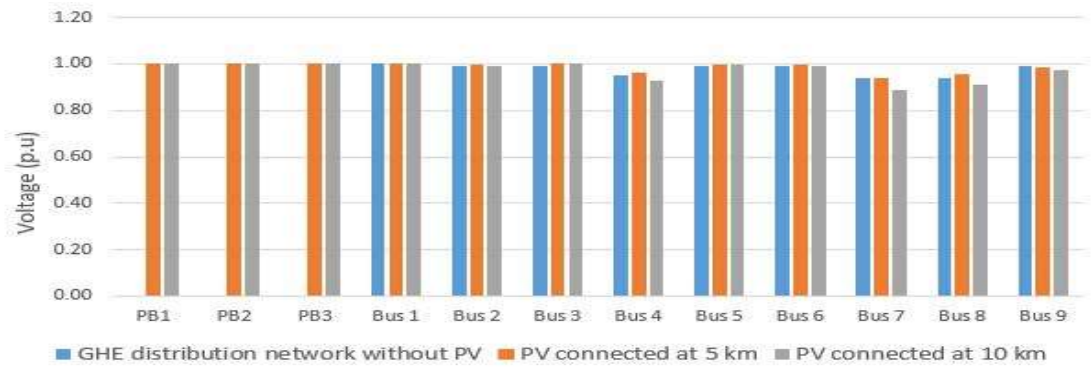

Figure 4.21: The impact of distance on voltage profile of PV connected GHE distribution network (PV connected to bus 7, 8 and 9).

iii. For the third scenario: PV system connected to bus 4

The result obtained is shown in Figure 4.22.

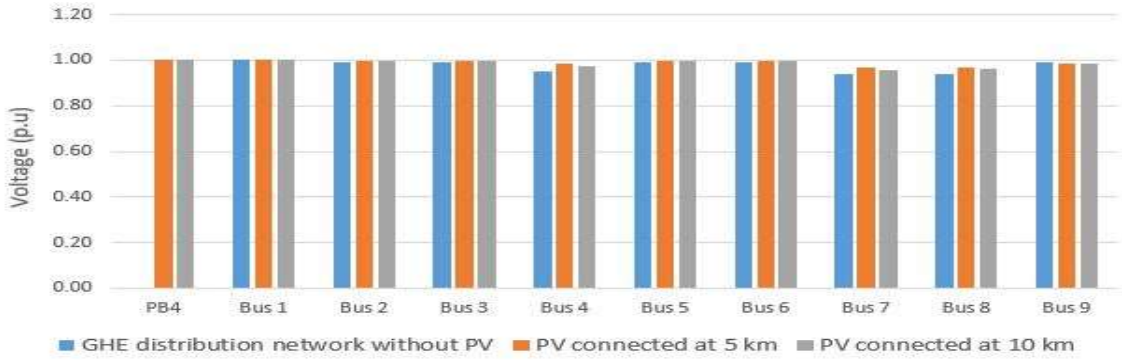

Figure 4.22: The impact of distance on voltage profile of PV connected GHE distribution network (PV connected to bus 4).

Expectedly, voltage drop also occurred as a result of the distances introduced. Buses 7 and 8 recorded 0.97p.u at 5 km and 0.96p.u at 10 km. However, no bus dropped below the lower limit of 0.95p.u.

4.4.2 Impact of distance between DG (PV) site and the load on fault level of the GHE distribution network

i. First scenario: PV systems connected to bus 7 and 8

The result of the load flow is shown in Figure 4.23.

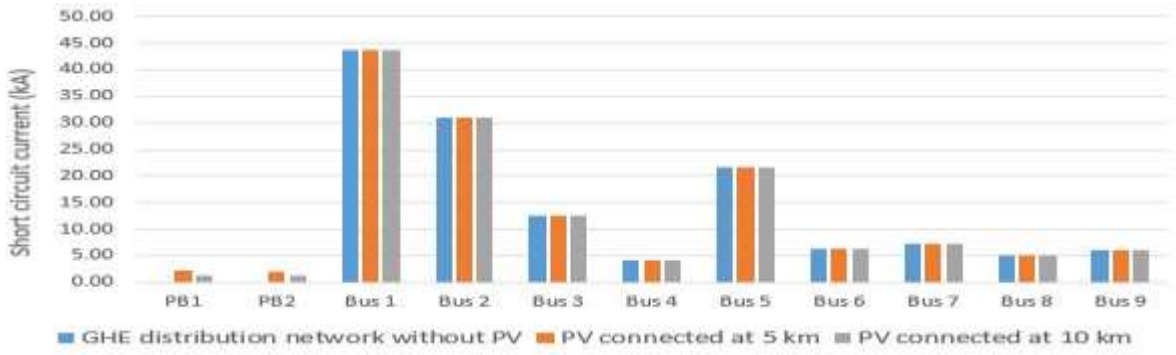

Figure 4.23: The impact of distance on fault level of PV connected distribution network (PV connected to bus 7 and 8)

The result showed no visible difference on the bus bars of the two networks except on the additional PV system bus bars (PB1 and PB2). The network did not suffer any significant

effect resulting from the distances of PV integration. PB1 and PB2 recorded 2.17kA and 1.93Ka at 5 km respectively. At 10 km, the magnitude of the fault on these bus bars were 1.28 kA and 1.19 kA respectively. It was observed that the fault magnitudes decreased as the distance between the PV and the load increased.

ii. Second scenario: PV systems connected to buses 7, 8 and 9

The result obtained is shown in Figure 4.24.

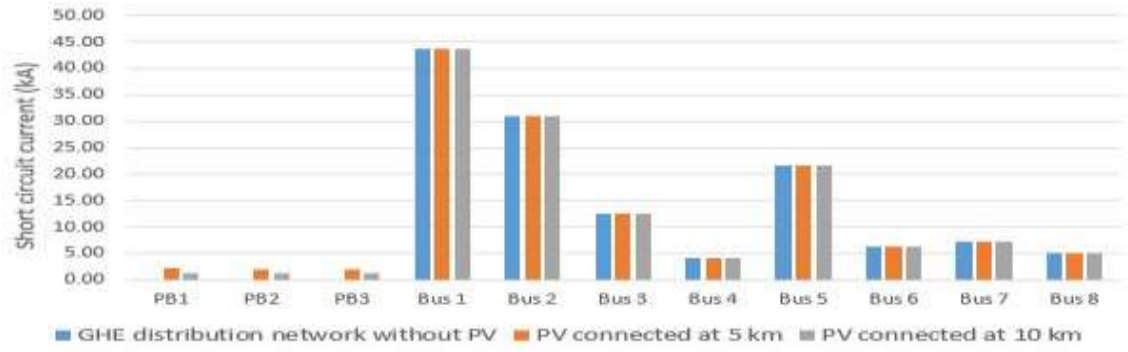

Figure 4.24: The impact of distance on fault level of PV connected distribution network (PV connected to bus 7, 8 and 9).

The result exhibited similar trend with the first scenario. The second scenario has on effect on the fault status of the network. However, PB3 recorded 2.04 kA and 1.23 kA at 5 km and 10 km respectively. The magnitude was more for the farther distance.

iii. Third scenario: PV system connected to bus 4

The result obtained is shown in Figure 4.25.

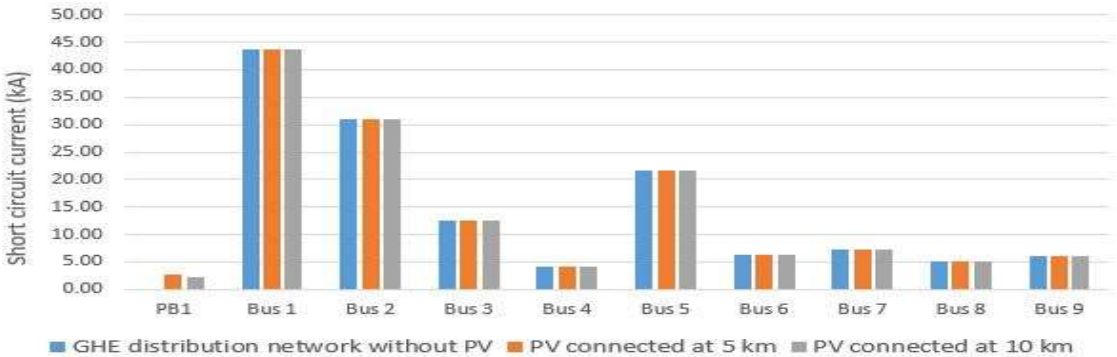

Figure 4.25: The impact of distance on fault level of PV connected distribution network (PV connected to bus 4).

The graph shows similar result with the two previous scenarios. However, larger magnitudes of fault on the PV bus (PB1), 2.82 kA and 2.16 kA at 5 km and 10 km respectively, were observed. This is could be attributed to the PV output, having about 15 parallel inverters as shown on Table 4.3.

4.4.3 Impact of distance between DG (PV) site and the load on line losses of the GHE distribution network.

i. First scenario: PV systems connected to bus 7 and 8

The result obtained is shown in Figure 4.26

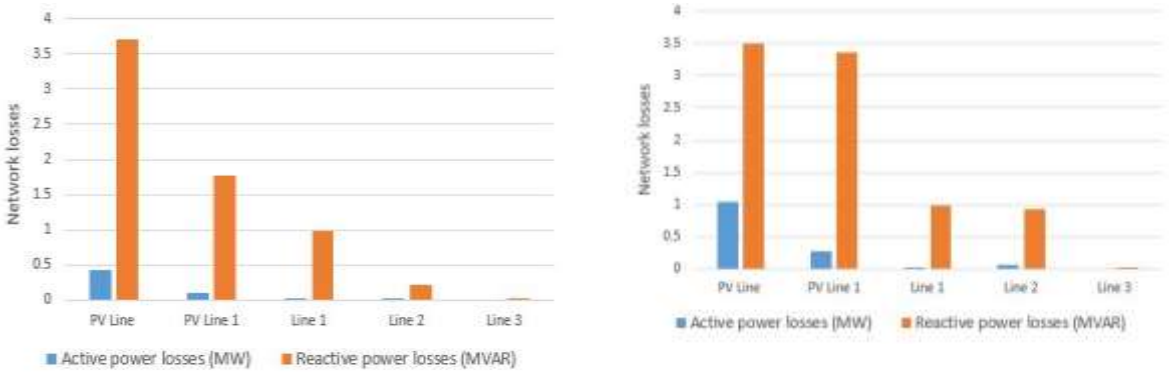

(a) (b)

Figure 4.26: The impact of distance on PV-connected GHE distribution network line losses at (a) 5 km and (b) 10 km (PV connected to buses 7 and 8)

Active power losses in the existing network were generally minimal due to the PV system's capacity as discussed earlier. Active power on Line 2 increased from 0.02 MW to 0.07 MW, from 5 km to 10 km respectively. However, reactive power losses were pronounced as seen from the graphs. Line 2 increased from 0.21 MVAR to 0.93 MVAR as the distance increased from 5 km to 10 km while lines 1 and 3 showed no significant difference. The PV lines recorded more losses due to maximum output of the PV systems supplying the network. Active power loss on PV line and PV line 1 were 0.42 MW and 0.1 MW at 5 km, and increased to 1.05 MW and 0.27 MW at 10 km respectively. The

reactive power losses were severely pronounced on the PV lines. PV line and PV line 1 increased from less than 1 MVAR to 3.71 MVAR and 1.77 MVAR respectively at a site distance of 5 km. Similarly, both lines increased to over 3 MVAR when the distance was increased to 10 km.

ii. For the second scenario: PV systems connected to bus 7, 8 and 9

The result obtained is shown in Figure 4.27

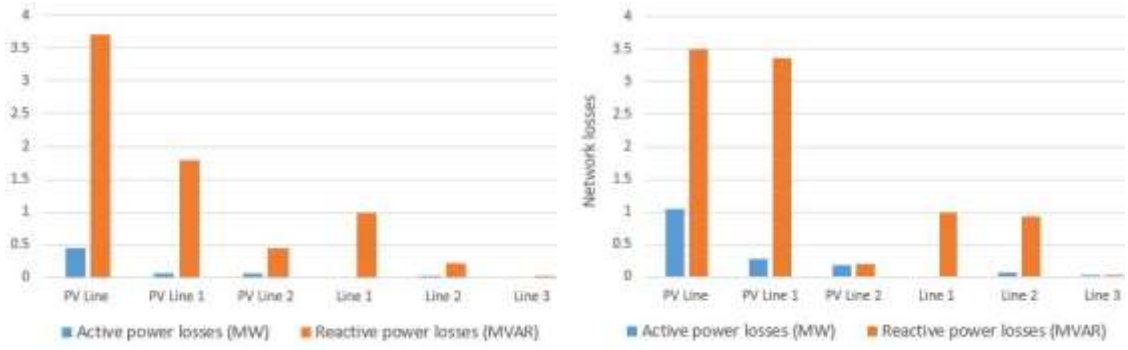

(a) (b)

Figure 4.27: The impact of distance on PV connected GHE distribution network line losses at (a) 5 km and (b) 10 km (PV connected to bus 7, 8 and 9)

Similar results were obtained with the additional PV line for this scenario, PV line 2. The line active power loss negligibly increased from 0.01 MW to 0.07 MW for both values of distance. The reactive power losses, though significant, were the same with the first scenario.

iii. Third scenario: PV system connected to bus 4

The result obtained is shown in Figure 4.28.

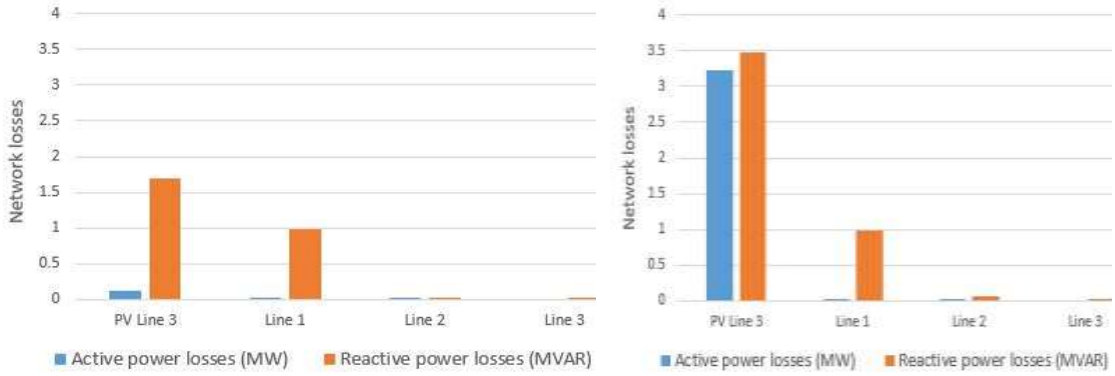

(a) (b)

Figure 4.28: The impact of distance on PV-connected GHE distribution network line losses at (a) 5 km and (b) 10 km (PV connected to bus 4)

The result showed a significant active power loss on the PV line 3 as the distance increased from 5 km to 10 km. At 5 km, the active power loss was 0.12 MW and rose to 3.22 MW at 10 km. Similarly, the reactive power loss on the PV line 3 increased from 1.70 MVAR to 3.47 MVAR. The remainder of the network showed no variant results from the previous scenarios.

4.4.4 Impact of distance between DG (PV) site and the load on thermal loading of the GHE distribution network

i. First scenario: PV systems connected to bus 7 and 8

The previous procedure that considers distance of PV site and the load was repeated to determine the network loading. The result obtained is graphically shown in Figure 4.29.

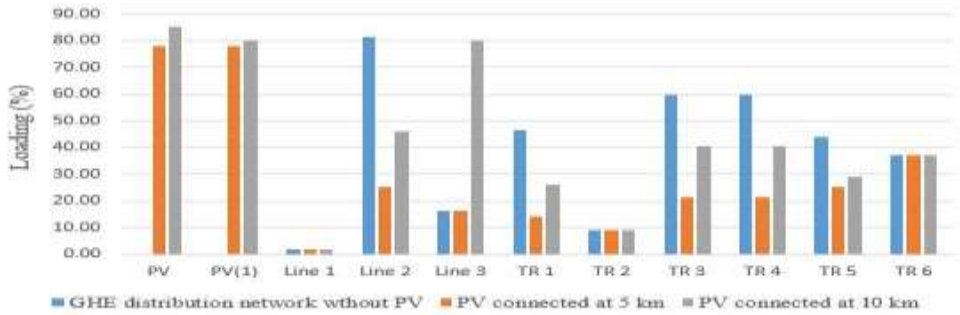

Figure 4.29: The impact of distance on thermal loading of PV-connected distribution network (PV connected to bus 7and 8).

From the result obtained, the loading of the network increased with the introduction of distance between the PV system and the load. For this scenario, the loading of line 2 increased to 25.44 % and 46.09 % at 5 km and 10 km respectively, from 9.29 % when distance was not considered. Generally, the loading of the network remain within acceptable limit despite the distance. However, line 3 became slightly overloaded (80.24 %) at 10 km. Furthermore, the PV lines (PV line and PV line 1) connected the PV sites with the load via bus 7 and 8, respectively, were heavily overloaded and the severity increased with distance. The PV line recorded 170.7 % and 186.69 % at 5 km and 10 km respectively, while PV line 1 was 85.33 % and 87.74 % load at 5 km and 10 km respectively. The PV outputs, PV and PV (1) were also overload with values 85.37 % and 80.24 % respectively at 10 km. Although, the focus of this research is on GHE distribution network, the huge loading of the PV lines was mitigated by paralleling the lines. Three paralleled lines of equal length, signifying the conventional 3phases, was introduced and the loading of the PV lines were reduced to acceptable values. PV line dropped to 56.3 % at 5 km and 56.5 % at 10 km. PV line 1 dropped to 28 % and and 28.3 % at 5 km and 10 km respectively. The PV outputs dropped to 76.8 % and 77.6 % respectively, at 10 km. Similarly, line 3 that was slightly overloaded, greatly reduced to 16.3 %. Therefore, the concern about the prohibited loading of the PV systems and their lines was solved.

ii. Second scenario: PV systems connected to bus 7, 8 and 9

The result is shown in Figure 4.30

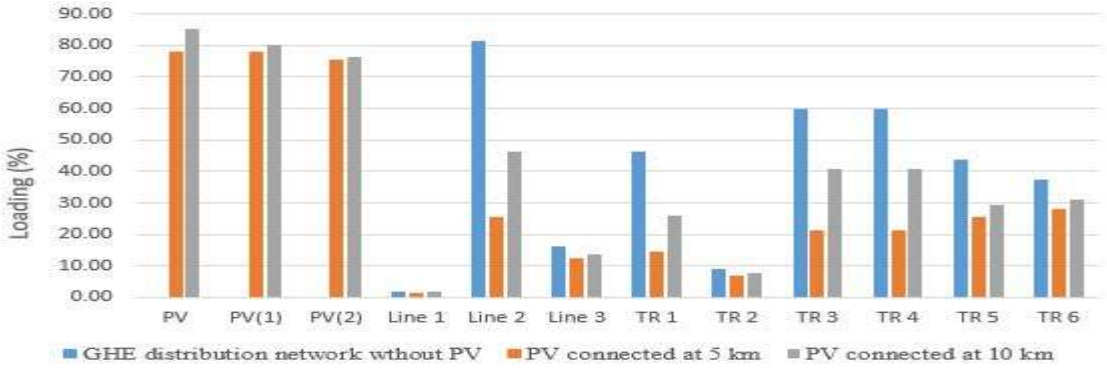

Figure 4.30: The impact of distance on thermal loading of PV connected GHE distribution network (PV connected to bus 7, 8 and 9).

The result shows no overload of the existing distribution network. Only the PV and the PV lines were slightly beyond the 80 % limit. These values were not as critical as in the first scenario, and the solution of paralleling the lines, already proffered and validated.

iii. Third scenario: PV system connected to bus 4

The same procedure was repeated for this scenario and the results obtained are shown in Figure 4.31.

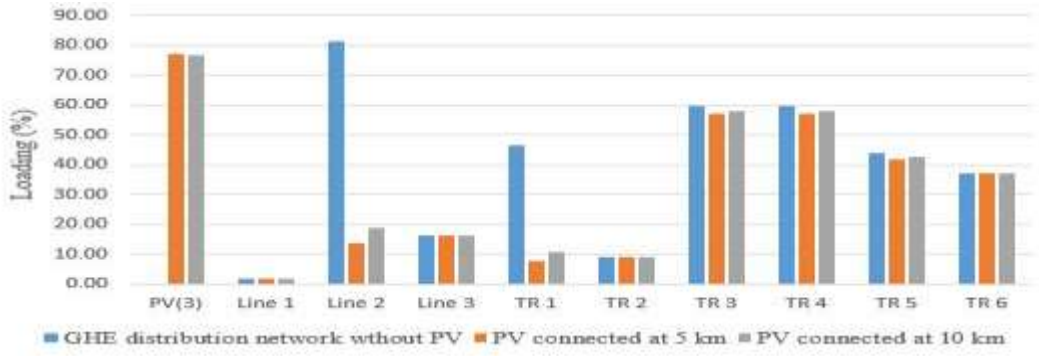

Figure 4.31: The impact of distance on thermal loading of PV connected GHE distribution network (PV connected to bus 4).

The third scenario shows no existing network equipment overload due to the distance between the PV site and the load. Even the PV output was not overloaded except the PV line 3 that was 84.2 % and 83.92 % at 5 km and 10 km respectively. As stated earlier, the current practice of 3phase paralleled transmission and distribution lines, was tested in the first scenario and validated to proffer solution to the overload.

4.5 Viability of the Research Findings

Solar energy is abundantly available around the chosen case study. An annual average solar radiation of 5.55 kWh/m^2/day was obtained, sufficient for efficient and sustained DG. The voltage profile of the utility distribution network was not adversely affected. Rather, it significantly improved with the connection of the PV system in conformity with the allowable limits of 0.95p.u to 1.05p.u, stipulated in the grid code for the Nigeria power system. The improvement was observed regardless of the PV system connection scenario and the distances introduced between the PV system and the load. Minor deviation could be addressed via the established voltage regulation techniques. The thermal loading of the network drastically reduced with additional power generation from the DG. Thus, the adverse effect of network overload is mitigated to less than the maximum 80 %, and this could preserve the system to the designed lifespan. The 3-phase paralleling the PV lines mitigated the significant loading of the lines. Furthermore, line losses slightly increased as expected but not outrageously. However, losses were minimized on the critical overloaded line due to reduction in loading with the connection of PV system. On the other hand, the inverter-based PV systems contributed no visible fault to the existing distribution network. Faults from the PV system were only significant on the PV bus bars and lines, which the power system protection schemes can handle.

Therefore, based on the conformity of the findings to the established designs, and the provisions of the grid code for the Nigeria power system, wheeling renewable energy from DG to diverse and stochastic residential load via the GHE Distribution Network for power supply improvement, is practicable and technically viable.

CHAPTER FIVE

5.0 CONCLUSION AND RECOMMENDATIONS

5.1 Conclusion

DG, off-grid or grid-tied, as an emerging component of a deregulated power system, improves consumer electricity supply. This emerging system in Nigeria, catalyzed by the Electric Power Sector Reform Act (EPSRA) 2005, is associated with wheeling which refers to transportation of energy from an IPP to a purchaser via the existing distribution network. While the overall aim is to improve power supply, the resultant network characteristics could be distorted. In this research study, the potentials and viability of renewable energy to meet the residential load demand of GHE, Abuja using HOMER software was determined. The can simulate, optimize and provide the best system configuration. Subsequently, DIgSILENT software was used to comparatively investigate the distribution network's voltage profile, fault level, line losses and thermal loading characteristics, with and without DG connections, thereby enabling wheeling energy to the diverse and stochastic residential load. The impact analysis was based on three scenarios of DG connection and distance between DG and the load. DIgSILENT has capability for modelling, simulation and is used to conduct grid-based DG network analysis efficiently.

The findings are presented as follows:

i. The geographical location of the case study has considerable potential for solar energy generation. The annual average solar radiation of 5.55 kWh/m^2/day was realized. On the other hand, the potential for wind energy resources was very low, with an annual average wind speed of 3.01 m/s at anemometer height of

50m. The wind speed fell short of the minimum of about 3.4 m/s at 10 m hub height required for viable energy generation. Furthermore, the wind turbine was not a component of the second most techno-economical configuration obtained from HOMER optimization. Thus, further study on wind energy generation was discontinued.

ii. The architecture of the optimal system is made of the grid, PV and converter with NPC and LCOE of $72.4 million and $0.0188 respectively, in realization of objective number 1 for this research study.

iii. The load flow of the distribution network conducted to ascertain the characteristics of the parameters shows that the voltages of bus 7 and 8 are below the allowable limit of 0.95p.u. Both buses are on 0.94p.u, and this could be attributed to the loading of line 2 that feeds the two buses, and also being among the farthest bus bars. Bus 4 which also feeds from the same line was on the lower voltage limit 0.95p.u, while the rest of the buses operates within the allowable limit of 0.95 to 1.05p.u. However, with PV connected to the distribution network, the voltage profile of the network improved to the allowable limit, for the three scenarios considered (For the first scenario, PV systems were connected to buses 7 and 8, and for the second, PV systems were connected to buses 7, 8 and 9. The third scenario had PV system connected to bus 4 only). The buses approximately recorded 1.00p.u, including the critical buses 7 and 8. Subsequently, the adverse effect of distance was observed on the voltage profile. The first and second scenarios were critical, as the voltage of bus 7 dropped to 0.94p.u at 5 km, and crashed to 0.89p.u at 10 km. Therefore, shorter distances, 5 km in this case, provides best voltage delivery to the load.

iv. The thermal loading of GHE distribution network was ascertained and it was observed that 33 kV Gwarinpa line, denoted as line 2, is 81.26 % loaded, against the maximum 80 %. This is not unexpected because the line is the most loaded among the lines feeding the estate case study. This state of line 2 could adversely affect the line losses as it does on voltage profile of the linked bus bars earlier stated. However, other network equipment such as the transformers and the lines were usually loaded. The highest value is 59.69 % on 15 MVA, 33/11 kV, TR 3 and TR 4, and the lowest value is 2.03 % on 132 kV Kubwa line (line 1).

However, with PV connected to the distribution network, the loading of the system reduced significantly. The critical line 2 dropped to an approximate value of 9 % under the three scenarios, while TR3 and TR4 reduced to 8.76 % under the first and second scenarios and 56.3 % under the third. On the other hand, distance reduced the improvement with PV connection. Line 2 increased to 25.44 % and 46.09 % at 5 km and 10 km respectively under the first and second scenarios.

v. Line losses were generally minimal as observed from the result obtained except on line 2. Active power losses were generally insignificant unlike with the reactive power loss. The reactive power loss was highest on line 2, with magnitude of 3.11 MVAR while the active power loss was 0.199 MW. However, with PV connected to the distribution network, reactive power losses on line 2 reduced significantly to 0.06 MVAR as a result of drastic reduction in loading. However, slight increases were observed, particularly on line 1 (0.99 MVAR). On the other hand, distance increased the losses slightly but significant on the PV lines.

vi. The fault level of the distribution network obtained from short circuit analysis, indicated highest magnitude of 43.74 kA on 132 kV bus 1, and lowest value of 4.04 kA on 33 kV bus 4. The 11 kV bus 7, 8 and 9 recorded 7.18 kA, 5.10 kA and 5.98 kA respectively. Despite connecting PV to the network, the magnitude of the short circuit currents are unchanged, and regardless of distance. However, fault currents were observed on the additional bus bars introduced at the DG site and the magnitudes decrease with distance.

vii. The integration of renewable DG for wheeling energy to GHE impacted positively on the existing distribution network voltage, thermal loading, line losses and fault level. The outcome of objective iii conforms to the characteristics of efficient power systems and therefore, affirms the viability of wheeling renewable DG to residential loads.

5.2 Recommendations

Based on the findings of this research study, the following recommendations were made:

i. Similar research study could be undertaken at geographical locations with viable potential for wind energy resources. Special types of turbines that requires less wind speed could also be considered for future study.

ii. Energy wheeling of renewable DG to multiple categories of consumers such as industrial and residential could be considered for future to determine its impact and viability on the resultant load characteristics.

5.3 Contributions to Knowledge

This thesis has contributed the following to knowledge:

i. Determination of the optimum hybrid renewable DG for Gwarinpa housing estate using HOMER.
ii. Simulation and load flow of the Gwarinpa housing estate's distribution network using DIgSILENT
iii. Determination of the impact of wheeling DG on the voltage profile (6.38 % improvement on the critical buses 7 and 8), thermal loading (overloaded state of line 2 relieved by 88.9 %) line losses (reduction of reactive power losses by 98% on line 2) and fault level of Gwarinpa housing estate's distribution network using DIgSILENT.
iv. Determination of the viability of wheeling renewable DG to residential loads via the existing distribution network infrastructure ascertained as the outcome of iii positively impacted the wheeling network.

REFERENCES

Adaramola, M. S. (2014). Viability of grid-connected solar PV energy system in Jos, Nigeria. *International Journal of Electrical Power & Energy Systems, 61*, 64-69.

Agbetuyi, A. F., Udeme, E. O., Obiakor, E., Kayode, O. O., & Owolabi, B. (2018). *Performance and Yield Assessment for Renewable Dispersed Generation in Nigeria: Case Study on Grid-Tied Solar PV Systems.* Paper presented at the IOP Conference Series: Materials Science and Engineering, *413*(1), 1-8.

Ahmadi, M. H., Ghazvini, M., Sadeghzadeh, M., Alhuyi Nazari, M., Kumar, R., Naeimi, A., & Ming, T. (2018). Solar power technology for electricity generation: A critical review. *Energy Science & Engineering, 6*(5), 340-361.

Ahmed, A., & Kunya, B. I. (2019). Investigation of Wind Energy Resource on the Basis of Weibull and Rayleigh Models in North Eastern and Western, Nigeria. *American Journal of Aerospace Engineering, 6*(1), 27-32.

Ahmed, M. F., & Gawad, A. F. A. (2016). *Utilization of Wind Energy in Green Buildings.* Paper presented at the Twelfth International Conference of Fluid Dynamics, Le Méridien Pyramids Hotel, Cairo, Egypt, 19-20.

Aika, T., Igbinovia, S., & Orukpe, P. (2020). Feasibility Assessment of Wind Energy Potential for Electricity Generation in Nigeria. *Jordan Journal of Electrical Engineering. All rights reserved-Volume, 6*(1), 25-34.

Ajayi, O. O., Fagbenle, R. O., Katende, J., Ndambuki, J. M., Omole, D. O., & Badejo, A. A. (2014). Wind energy study and energy cost of wind electricity generation in nigeria: Past and recent results and a case study for south west nigeria. *Energies, 7*(12), 8508-8534.

Akinyele, D. (2017). Techno-economic design and performance analysis of nanogrid systems for households in energy-poor villages. *Sustainable cities and society, 34*, 335-357.

Al Ghaithi, H. M., Fotis, G. P., & Vita, V. (2017). Techno-economic assessment of hybrid energy off-grid system—A case study for Masirah island in Oman. *International Journal of Power and Energy Research, 1*, 103-116.

Al Momani, T., Harb, A., & Amoura, F. (2017). *Impact of photovoltaic systems on voltage profile and power losses of distribution networks in jordan.* Paper presented at the 2017 8th International Renewable Energy Congress (IREC), 1-6.

Alao, A. A. (2016). Residential and Industrial Electricity Consumption Dynamics and Economic Growth in Nigeria 1980-2010. *International Journal of Economy, Energy and Environment, 1*(3), 55-63.

Annapolis, M. D. (2020). *Wind Turbines*. Lakewood, United State: CFD Open Series.

Aoun, N., & Bailek, N. (2019). Evaluation of mathematical methods to characterize the electrical parameters of photovoltaic modules. *Energy Conversion and Management, 193*, 25-38.

Areo, I., Sako, K. C., & Lucky, E. (2019). Assessment of Public Restroom Distribution Pattern in Gwarinpa, Federal Capital City;(FCC) Abuja. *Confluence Journal of Environmental Studies, 13*(1), 12-22.

Ayadi, O., Al-Assad, R., & Al Asfar, J. (2018). Techno-economic assessment of a grid connected photovoltaic system for the University of Jordan. *Sustainable cities and society, 39*, 93-98.

Ayodele, T., & Ogunjuyigbe, A. (2015). Wind energy resource, wind energy conversion system modelling and integration: a survey. *International Journal of Sustainable Energy, 34*(10), 657-671.

Ayodele, T., Ogunjuyigbe, A., Odigie, O., & Jimoh, A. (2018). On the most suitable sites for wind farm development in Nigeria. *Data in brief, 19*, 29-41.

Azerefegn, T. M., Bhandari, R., & Ramayya, A. V. (2020). Techno-economic analysis of grid-integrated PV/wind systems for electricity reliability enhancement in Ethiopian industrial park. *Sustainable Cities and Society, 53*, 1-32.

Azodo, A. P. (2014). Electric power supply, main source and backing: A survey of residential utilization features. *International Journal of Research Studies in Management, 3*(2), 87-102.

Babatunde, M. A., & Shuaibu, M. I. (2009). *The demand for residential electricity in Nigeria: a bound testing approach.* Paper presented at the Proceedings of 2nd International Workshop on Empirical Methods in Energy Economics, Zurich, Switzerland, 1-16.

Baji, V., & Ashok, S. (1998). Wheeling power—a case study in India. *International Journal of Electrical Power & Energy Systems, 20*(5), 333-336.

Barzegkar-Ntovom, G. A., Chatzigeorgiou, N. G., Nousdilis, A. I., Vomva, S. A., Kryonidis, G. C., Kontis, E. O., Georghiou, G. E., Christoforidis, G. C., & Papagiannis, G. K. (2020). Assessing the viability of battery energy storage systems coupled with photovoltaics under a pure self-consumption scheme. *Renewable Energy, 152*, 1302-1309.

Basher, M., Hossain, M. K., & Akand, M. (2019). Effect of surface texturization on minority carrier lifetime and photovoltaic performance of monocrystalline silicon solar cell. *Optik, 176*, 93-101.

Bhutta, M. M. A., Hayat, N., Farooq, A. U., Ali, Z., Jamil, S. R., & Hussain, Z. (2012). Vertical axis wind turbine–A review of various configurations and design techniques. *Renewable and Sustainable Energy Reviews, 16*(4), 1926-1939.

Bilal, M., Ullah, R., Ali, A., Khan, M. H., & Ullah, Z. (2016). *Wheeling hybrid energy system for industries.* Paper presented at the 2016 International Conference on Computing, Electronic and Electrical Engineering (ICE Cube), 169-174.

Bohlmann, J. A., & Inglesi-Lotz, R. (2018). Analysing the South African residential sector's energy profile. *Renewable and Sustainable Energy Reviews, 96*, 240-252.

Cagnazzi, A. (2020). *The photovoltaic, a driving force for the new green deal.* (Master of Science), Selinus University of Sciences and Literature, Delaware, USA.

Chen, H., Huang, Y., Shen, H., Chen, Y., Ru, M., Chen, Y., Lin, N., Su, S., Zhuo, S., & Zhong, Q. (2016). Modeling temporal variations in global residential energy consumption and pollutant emissions. *Applied Energy, 184*, 820-829.

Chen, Y.-T. (2017). The factors affecting electricity consumption and the consumption characteristics in the residential sector—A case example of Taiwan. *Sustainability, 9*(8), 1484.

Dahiru, A. T., & Tan, C. W. (2020). Optimal sizing and techno-economic analysis of grid-connected nanogrid for tropical climates of the Savannah. *Sustainable Cities and Society, 52*(2020), 1-12.

Diawuo, F. A., Sakah, M., Pina, A., Baptista, P. C., & Silva, C. A. (2019). Disaggregation and characterization of residential electricity use: Analysis for Ghana. *Sustainable Cities and Society, 48*(2019), 1-16.

Durmaz, T., Pommeret, A., & Tastan, H. (2020). Estimation of residential electricity demand in Hong Kong under electricity charge subsidies. *Energy Economics, 88*(2020), 1-15.

Dyak, A., Abu-Lehyeh, E., & Kiwan, S. (2016). *Techno-economic assessment of integrating renewable energy on the electricity grid in jordan*. Paper presented at the GCREEDER 2016, Amman-Jordan.

El-Khattam, W., & Salama, M. M. (2004). Distributed generation technologies, definitions and benefits. *Electric power systems research, 71*(2), 119-128.

Emovon, I., Samuel, O. D., Mgbemena, C. O., & Adeyeri, M. K. (2018). Electric Power generation crisis in Nigeria: A Review of causes and solutions. *International Journal of Integrated Engineering, 10*(1), 45-56.

Ezenugu, I. A., Nwokonko, S. C., & Markson, I. (2017). Modelling and Forecasting of residential electricity consumption in Nigeria using Multiple and Quadratic regression models. *American Journal of Software Engineering and Applications, 6*(3), 99-104.

Figgener, J., Stenzel, P., Kairies, K.-P., Linßen, J., Haberschusz, D., Wessels, O., Angenendt, G., Robinius, M., Stolten, D., & Sauer, D. U. (2020). The development of stationary battery storage systems in Germany–A market review. *Journal of Energy Storage, 29*, 1-20.

Gugul, G. N., & Koksal, M. A. (2017). *Some Insights to the Lighting Electricity Consumption of Turkish Households.* Paper presented at the Energy Efficiency in Domestic Appliances and Lighting (EEDAL'17), *3*, 1-429.

Guo, Z., Zhou, K., Zhang, C., Lu, X., Chen, W., & Yang, S. (2018). Residential electricity consumption behavior: Influencing factors, related theories and intervention strategies. *Renewable and Sustainable Energy Reviews, 81*, 399-412.

Hansen, A. D., Iov, F., Sørensen, P. E., Cutululis, N. A., Jauch, C., & Blaabjerg, F. (2003). Dynamic wind turbine models in power system simulation tool DIgSILENT. In R. Risø National Laboratory (Ed.), (pp. 1-80). Roskilde: Risø National Laboratory and Aalborg University.

Happ, H. (1994). Cost of wheeling methodologies. *IEEE Transactions on Power systems, 9*(1), 147-156.

Idowu, S. S., Ibietan, J., & Olukotun, A. (2019). Nigeria's Electricity Power Sector Reform: An Appraisal of Unresolved Issues. *International Journal of Energy Economics and Policy, 9*(6), 336-341.

Imam, A. A., & Al-Turki, Y. A. (2020). Techno-Economic Feasibility Assessment of Grid-Connected PV Systems for Residential Buildings in Saudi Arabia—A Case Study. *Sustainability, 12*(1), 201-262.

Infield, D., & Freris, L. (2020). *Renewable energy in power systems*: John Wiley & Sons.

Johari, M., Jalil, M., & Shariff, M. F. M. (2018). Comparison of horizontal axis wind turbine (HAWT) and vertical axis wind turbine (VAWT). *International Journal of Engineering and Technology, 7*(4.13), 74-80.

Kalappan, B., Amudha, A., & Keerthivasan, K. (2020). Techno-economic study of hybrid renewable energy system of Metropolitan Cities in India. *International Journal of Ambient Energy*, 1-5.

Kale, A. S., Nemeth, W., Guthrey, H., Kennedy, E., Norman, A. G., Page, M., Al-Jassim, M., Young, D. L., Agarwal, S., & Stradins, P. (2019). Understanding the charge transport mechanisms through ultrathin SiO x layers in passivated contacts for high-efficiency silicon solar cells. *Applied Physics Letters, 114*(8), 1-6.

Kavaklioglu, K. (2019). Principal components based robust vector autoregression prediction of Turkey's electricity consumption. *Energy Systems, 10*(4), 889-910.

Kewo, A., Manembu, P. D., & Nielsen, P. S. (2020). Synthesising Residential Electricity Load Profiles at the City Level Using a Weighted Proportion (Wepro) Model. *Energies, 13*(14), 1-29.

Khetrapal, P. (2020). Distributed Generation: A critical review of technologies, grid integration issues, growth drivers and potential benefits. *International Journal of Renewable Energy Development, 9*(2), 189-205.

Krishnamoorthy, M., Raj, P. A. D. V., Suresh, S., & Natarajan, K. (2020). Techno Economic Analysis of Hybrid Renewable Electrification System in Different Climatic Zones *Emerging Trends in Electrical, Communications, and Information Technologies* (pp. 151-166): Springer.

Kucevic, D., Tepe, B., Englberger, S., Parlikar, A., Mühlbauer, M., Bohlen, O., Jossen, A., & Hesse, H. (2020). Standard battery energy storage system profiles: Analysis of various applications for stationary energy storage systems using a holistic simulation framework. *Journal of Energy Storage, 28*(10), 1-21.

Kumar, P., & Deokar, S. (2018). *Optimal design configuration using HOMER.* Paper presented at the Advances in Systems, Control and Automation, *24*(2016), 499-504.

Kumar, R., Raahemifar, K., & Fung, A. S. (2018). A critical review of vertical axis wind turbines for urban applications. *Renewable and Sustainable Energy Reviews, 89*, 281-291.

Kumari, J., Subathra, P., Moses, J. E., & Shruthi, D. (2017). *Economic analysis of hybrid energy system for rural electrification using HOMER.* Paper presented at the 2017 International Conference on Innovations in Electrical, Electronics, Instrumentation and Media Technology (ICEEIMT), 151-156.

Lee, W.-J., Lin, C., & Swift, K. (2001). Wheeling charge under a deregulated environment. *IEEE Transactions on industry applications, 37*(1), 178-183.

Li, B., Robinson, D. A., & Agalgaonkar, A. (2017). *Identifying the wheeling costs associated with solar sharing in LV distribution networks in Australia using power flow tracing and MW-Mile methodology.* Paper presented at the 2017 Australasian Universities Power Engineering Conference (AUPEC), 1-6.

Lin, B., & Wang, Y. (2020a). Does energy poverty really exist in China? From the perspective of residential electricity consumption. *Energy Policy, 143*, 111557.

Lin, B., & Wang, Y. (2020b). Does energy poverty really exist in China? From the perspective of residential electricity consumption. *Energy Policy, 143*(8), 1-10.

Lin, B., & Zhu, J. (2020). Chinese electricity demand and electricity consumption efficiency: Do the structural changes matter? *Applied Energy, 262*, 114505.

Lipu, M. S. H., Hafiz, M. G., Ullah, M. S., Hossain, A., & Munia, F. Y. (2017). Design optimization and sensitivity analysis of hybrid renewable energy systems: A case of Saint Martin Island in Bangladesh. *international journal of renewable energy research, 7*(2), 988-998.

Ma, X., Wang, M., & Li, C. (2020). A Summary on Research of Household Energy Consumption: A Bibliometric Analysis. *Sustainability, 12*(1), 316.

Magarappanavar, U. S., & Koti, S. (2016). Optimization of Wind-Solar-Diesel Generator Hybrid Power System using HOMER. *Optimization, 3*(06), 522-526.

Marinić-Kragić, I., Vučina, D., & Milas, Z. (2019). Concept of flexible vertical-axis wind turbine with numerical simulation and shape optimization. *Energy, 167*, 841-852.

Marion, B., Adelstein, J., Boyle, K. e., Hayden, H., Hammond, B., Fletcher, T., Canada, B., Narang, D., Kimber, A., & Mitchell, L. (2005). *Performance parameters for grid-connected PV systems.* Paper presented at the Conference Record of the Thirty-first IEEE Photovoltaic Specialists Conference, 2005., 1601-1606.

Mercado, K. D., Jiménez, J., & Quintero, M. C. G. (2016). *Hybrid renewable energy system based on intelligent optimization techniques.* Paper presented at the 2016 IEEE International Conference on Renewable Energy Research and Applications (ICRERA), 661-666.

Mexis, I., & Todeschini, G. (2020). Battery Energy Storage Systems in the United Kingdom: A Review of Current State-of-the-Art and Future Applications. *Energies, 13*(14), 1-31.

Momoh, J. (2019). *Nigeria Electricity Regulatory Commission's role in the availability of electricity in Nigeria.* Paper presented at the IEEE Africa conference, Abuja, Nigeria, *10*(5), 1-7.

Murray, W., & Adonis, M. (2019). *Efficacy of Energy Wheeling to Endorse Renewable Energy Generation.* Paper presented at the AIUE Proceedings of the 17th Industrial and Commercial Use of Energy (ICUE) Conference, Cape Town, 1-8.

Murray, W. N. (2018). *Energy wheeling viability of distributed renewable energy for industry.* (Master of Engineering), Cape Peninsula University of Technology.

Nassar, I. A., Seif, M. S., & Elattar, M. M. (2020). Improving the voltage quality of Abu Hummus network in Egypt. *International Journal of Electrical and Computer Engineering, 10*(5), 4458-4468.

Negi, S., & Mathew, L. (2014). Hybrid renewable energy system: a review. *International Journal of Electronic and Electrical Engineering, 7*(5), 535-542.

Nemeth-Durko, E., Juhasz, P., & Dudas, F. (2020). *Forecasting Residential Electricity Consumption Based On Urbanization And Income Projections.* Paper presented at the ECMS, 104-110.

NERC. (2018). *The Grid Code for the Nigeria Electricity Transmission System*.

Nnodu, V., Obiegbu, M., & Eneche, P. (2017). An Assessment of Sustainable Energy-efficient Strategies for Retrofitted Building Development in Abuja, Nigeria. *Archives of Current Research International*, 1-12.

Nwachukwu, M. U., Ezedinma, N. F., & Jiburum, U. (2014). Comparative Analysis of Electricity Consumption among Residential, Commercial and Industrial Sectors of the Nigeria s Economy. *Journal of Energy Technologies and Policy, 4*(3), 1-7.

Olanipekun, B. A., & Adelakun, N. O. (2020). Assessment of Renewable Energy in Nigeria: Challenges and Benefits. *International Journal of Engineering Trends and Technology (IJETT), 68*(1), 64-67.

Olaniyan, K., McLellan, B., Ogata, S., & Tezuka, T. (2018). Estimating residential electricity consumption in Nigeria to support energy transitions. *Sustainability, 10*(1440), 1-22.

Olanrewaju, S., Olafioye, S., & Oguntade, E. (2020). Modelling Nigeria Population Growth: A Trend Analysis Approach. *International Journal of Innovative Science and Research Technology, 5*(4), 52-64.

Olaoye, T., Ajilore, T., Akinluwade, K., Omole, F., & Adetunji, A. (2016). Energy crisis in Nigeria: Need for renewable energy mix. *American Journal of Electrical and Electronic Engineering, 4*(1), 1-8.

Olatomiwa, L. (2016a). Optimal configuration assessments of hybrid renewable power supply for rural healthcare facilities. *Energy Reports, 2*, 141-146.

Olatomiwa, L., Blanchard, R., Mekhilef, S., & Akinyele, D. (2018). Hybrid renewable energy supply for rural healthcare facilities: An approach to quality healthcare delivery. *Sustainable Energy Technologies and Assessments, 30*, 121-138.

Olatomiwa, L., & Blanchard, R. E. (2019,). *Maximizing the penetration levels of hybrid renewable energy systems in rural areas with demand side management approaches in achieving SDGs.* Paper presented at the International Conference on Energising the Sustainable Development Goals through Appropriate Technology and Governance, De-Montfort University, Leicester, United Kingdom. 4-5th July 2019 pp.88-99. https://dora.dmu.ac.uk/handle/2086/18646, 88-99.

Olatomiwa, L., Mekhilef, S., Huda, A., & Sanusi, K. (2015). Techno-economic analysis of hybrid PV–diesel–battery and PV–wind–diesel–battery power systems for mobile BTS: the way forward for rural development. *Energy Science & Engineering, 3*(4), 271-285.

Olatomiwa, L. J. (2016b). *Optimal planning and design of hybrid renewable energy system for rural healthcare facilities.* (Degree of Doctor of Philosophy), University of Malaya, Kuala Lumpur.

Olomiyesan, B., Oyedum, O., Ugwuoke, P., & Abolarin, M. (2017). Assessment of wind energy resources in Nigeria–a case study of north-western region of Nigeria. *Int J Phys Res, 5*(2), 83-90.

Owoeye, S., Waheed, A., Ishola, A., & Yussouf, A. (2017). Modelling a wind map of nigeria to assess the utilization of wind as an alternetive source of energy. *LAUTECH Journal of Engineering and Technology, 11*(2), 24-33.

Owusu, P. A., & Asumadu-Sarkodie, S. (2016). A review of renewable energy sources, sustainability issues and climate change mitigation. *Cogent Engineering, 3*(1), 1-14.

Oyedepo, S. O. (2019). Energy Use and Energy Saving Potentials in Food Processing and Packaging: Case Study of Nigerian Industries *Bottled and Packaged Water* (pp. 423-452): Elsevier.

Purohit, I., & Purohit, P. (2018). Performance assessment of grid-interactive solar photovoltaic projects under India's national solar mission. *Applied Energy, 222*, 25-41.

Radzi, M. A. M., Rahim, N. A., Che, H. S., Ohgaki, H., Farzaneh, H., Wong, W. S. H., & Hung, L. C. (2019). Optimal solar powered system for long houses in sarawak by using homer tool. *ASEAN Engineering Journal, 9*(1), 1-14.

Ramanathan, R. (2019). *Impact of Variable Energy Resources on Energy Imbalance Markets and Wheeling Transactions.* Paper presented at the 2019 IEEE PES GTD Grand International Conference and Exposition Asia (GTD Asia), 148-152.

Sachs, J., Moya, D., Giarola, S., & Hawkes, A. (2019). Clustered spatially and temporally resolved global heat and cooling energy demand in the residential sector. *Applied Energy, 250*, 48-62.

Santosa, B., & Rusdiansyah, A. (2018). *Cost analysis of an electricity supply chain using modification of price based dynamic economic dispatch in wheeling transaction scheme.* Paper presented at the IOP Conference Series: Materials Science and Engineering, *337*(1), 1-8.

Saxena, A., Pandey, S. N., & Srivastava, L. (2016). *Genetic algorithm based wheeling prices allocation for Indian power utility by using MVA-mile and MW-mile approaches.* Paper presented at the 2016 International Conference on Emerging Trends in Electrical Electronics & Sustainable Energy Systems (ICETEESES), 60-63.

Sood, Y. R., Padhy, N. P., & Gupta, H. O. (2002). Wheeling of power under deregulated environment of power system-a bibliographical survey. *IEEE Transactions on Power systems, 17*(3), 870-878.

Su, Y.-W. (2020). Residential electricity demand in Taiwan: the effects of urbanization and energy poverty. *Journal of the Asia Pacific Economy*, 1-24.

Sultan, H. M., Diab, A. A. Z., Kuznetsov, O. N., Ali, Z. M., & Abdalla, O. (2019). Evaluation of the impact of high penetration levels of PV power plants on the capacity, frequency and voltage stability of Egypt's unified grid. *Energies, 12*(3), 552-560.

Taale, F., & Kyeremeh, C. (2019). Drivers of households' electricity expenditure in Ghana. *Energy and Buildings, 205*(8), 546-552.

To, W.-M., Lee, P. K. C., & Lai, T.-M. (2017). Modeling of monthly residential and commercial electricity consumption using nonlinear seasonal models—The case of Hong Kong. *Energies, 10*(7), 885.

Tukur, M. U., & Solomon, O. I. (2019). Impact of Deregulation on Residential Electricity Consumption in Nigeria: 1980-2017. *International Journal of Academic Research in Business and Social Sciences, 9*(6), 163-184.

Tummala, A., Velamati, R. K., Sinha, D. K., Indraja, V., & Krishna, V. H. (2016). A review on small scale wind turbines. *Renewable and Sustainable Energy Reviews, 56*, 1351-1371.

Uzoh, A., Nwaru, N., & Anyanwu, F. Effect of Electricity Power Consumption on Economic Growth of Nigeria. *International Journal of Economic Development Research and Investment, 7*(3), 165-178.

Wang, S., Liu, H., Pu, H., & Yang, H. (2020). Spatial disparity and hierarchical cluster analysis of final energy consumption in China. *Energy, 197*, 1-11.

Wen, L., & Yuan, X. (2020). Forecasting the annual household electricity consumption of Chinese residents using the DPSO-BP prediction model. *Environmental Science and Pollution Research*, 1-19.

Weng, D. (2016). *Microgrid Techno-Economic Assessment Presentation.* Paper presented at the IRED Conference, Niagara Falls, 1-43.

Xin-gang, Z., & Pei-ling, L. (2020). Is the energy efficiency improvement conducive to the saving of residential electricity consumption in China? *Journal of Cleaner Production, 249*(10), 1-37.

Yang, Y., Bremner, S., Menictas, C., & Kay, M. (2018). Battery energy storage system size determination in renewable energy systems: A review. *Renewable and Sustainable Energy Reviews, 91*, 109-125.

Zaidi, B., Saouane, I., & Shekhar, C. (2018). Simulation of single-diode equivalent model of polycrystalline silicon solar cells. *International Journal of Materials Science and Applications, 7*(1), 8-10.

Zhang, X., & Zhu, S. (2021). Distributed energy trading with transmission cost: a Stackelberg game approach. *Science China Information Sciences, 64*, 1-3.